Analyst

ROYAL SOCIETY OF CHEMISTRY

TUTORIAL REVIEW

View Article Online
View Journal | View Issue

Cite this: *Analyst*, 2021, **146**, 2784

Smartphone-based colorimetric detection systems for glucose monitoring in the diagnosis and management of diabetes

Özlem Kap, [a] Volkan Kılıç, [b] John G. Hardy [c,d] and Nesrin Horzum *[a]

Received 13th October 2020,
Accepted 11th March 2021

DOI: 10.1039/d0an02031a

rsc.li/analyst

Diabetes is a group of metabolic conditions resulting in high blood sugar levels over prolonged periods that affects hundreds of millions of patients worldwide. Measuring glucose concentration enables patient-specific insulin therapy, and is essential to reduce the severity of the disease, potential complications, and related mortalities. Recent advances and developments in smartphone-based colorimetric glucose detection systems are discussed in this review. The importance of glucose monitoring, data collection, transfer, and analysis, *via* non-invasive/invasive methods is highlighted. The review also presents various approaches using 3D-printed materials, screen-printed electrodes, polymer templates, designs allowing multiple glucose analysis, bioanalytes and/or nanostructures for glucose detection. The positive effects of advances in improving the performance of smartphone-based platforms are introduced along with future directions and trends in the application of emerging technologies in smartphone-based diagnostics.

1. Introduction

Diabetes mellitus, generally known as diabetes, is a metabolic disorder that results in high blood glucose levels. The main types of diabetes are Type 1, Type 2, and gestational which arise from damage to insulin-producing cells, insulin production deficiency of the pancreas, and high blood glucose levels during pregnancy, respectively. According to the World Health Organization (WHO), diabetes causes 1.6 million deaths every year,[1] and it is, therefore, important to follow the blood sugar level of patients accurately since a complete cure is not yet possible.

The history of monitoring methods, illustrated in Fig. 1, dates back over one hundred years with the copper reagent developed by Benedict to detect urine glucose. The subsequent development of various other products (such as Clinitest®, Tes-tape roll®, Clinistix®, *etc.*) enables the determination of urine glucose *via* analysis of the differences in color.[2] Clark and Lyons subsequently incorporated the enzymatic reaction with glucose oxidase (GOx) in an electrochemical cell as an electrochemical detector to measure the oxygen concentration which is proportional to the glucose concentration.[3] A whole blood glucose determination could be performed with Dextrostix®, test strips charting color differences depending on the concentration, and these strips were converted into numerical data using an Ames reflectometer as a self-monitoring system.[4]

The Biostator system®, which is an artificial pancreas combining an intravenous glucose sensor and insulin/dextrose pump, acted as a continuous monitoring system for blood glucose.[5–7] A Yellow Springs Instrument (Model 23A YSI analyzer) has been produced commercially that allows glucose analysis from whole blood using Clark's enzymatic biosensor technology. NovoPen®, was the first insulin pen for painless and straightforward daily treatment launched in 1985. A self-monitoring blood glucose pen-meter biosensor was developed by MediSense in 1987 based on the enzymatic electrochemical measurement on a disposable strip.[8] It is important to note that it is impractical to identify blood glucose by finger-pricking accurately. Therefore, the subcutaneously insertable MiniMed™ which provides three days of reliable operation was developed in 1999.[9] In 2000, the glucose measurement evolution was improved from *in vivo* continuous glucose monitoring to wearable non-invasive Glucowatch Biographer®,[10] a wristwatch using reverse iontophoresis on an electrochemical electrode system. Due to the importance of monitoring the glucose level and increasing awareness of the patient, the use

[a]*Department of Engineering Sciences, İzmir Katip Çelebi University, 35620 Turkey. E-mail: nesrin.horzum.polat@ikcu.edu.tr; Fax: +90 232 325 33 60; Tel: +90 232 329 35 35*
[b]*Department of Electrical and Electronics Engineering, İzmir Katip Çelebi University, 35620 Turkey*
[c]*Department of Chemistry, Lancaster University, Lancaster, Lancashire LA1 4YB, UK*
[d]*Materials Science Institute, Lancaster University, Lancaster, Lancashire LA1 4YB, UK*

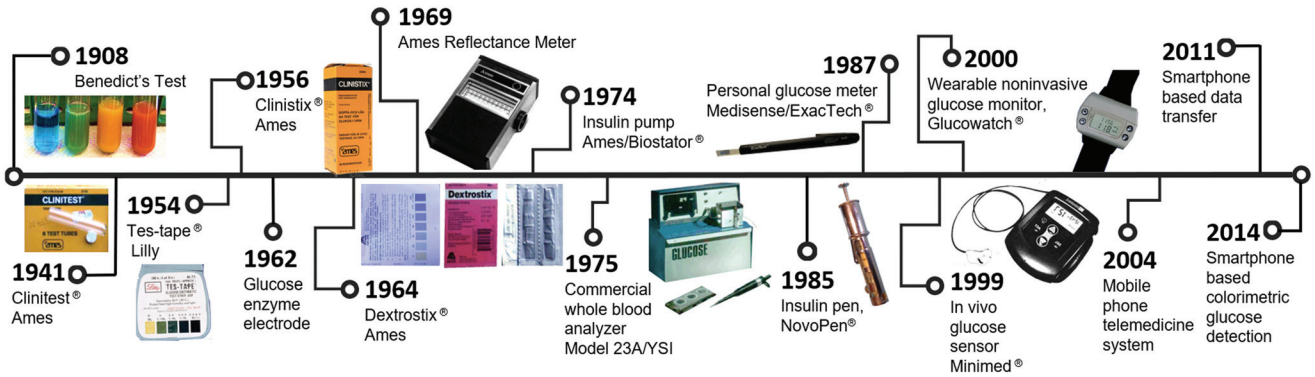

Fig. 1 Timeline of the diabetes screening and management systems from past to present.

of advanced technology has become widespread in glucose management for both informative and data transfer purposes *via* text messages and smartphone applications.[11–17] As it can be seen in Fig. 2, the number of papers based on smartphone-based diabetes management and glucose detection studies has increased with the introduction of smartphones into daily life over the last decade. Although both management and determination studies are trending, the management-related ones are somewhat more prevalent due to the wide use of mobile devices and applications for healthcare.

Smartphone-based glucose monitors use either blood or body fluids such as sweat, tears, urine, saliva, and interstitial fluid (ISF). There are several smartphone-based blood glucose monitors in the market including GlucoWise™,[18] DiaMonTech,[19] and OrSense's NBM-200G.[20] In addition, Dexcom G6, Abbott Freestyle Libre, the FibreSense system from EyeSense GmbH, Eversense XL by Senseonics, BIORASIS Glucowizzard, and SugarBEAT® by Nemaura Medical, Medtronic have been released for interstitial fluid glucose monitoring.[21] The technology used in these platforms is mainly based on spectroscopy, transdermal extraction, fluorescence, electromagnetic sensing, and polarimetry. On the other hand, measuring glucose from body fluids instead of blood still remains expensive and complicated. Furthermore, accuracy, safety, selectivity, sensitivity, stability and measurement time of the underlying technologies pose key challenges. The difficulties in the existing technologies and the recent advances in the field of smartphone technology have led to the development of cheaper smart glucometers capable of detecting threshold concentration ranges with high accuracy and selectivity.[22]

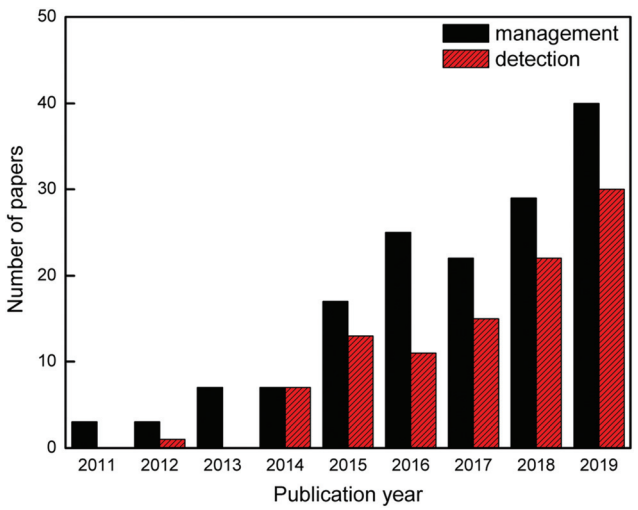

Fig. 2 The number of publications in a given year in the Web of Science (WOS) database using the keywords; 'Glucose and smartphone' are classified as 'management' and 'detection'.

Nevertheless, there are some drawbacks to overcome for the widespread operation of smartphones in colorimetric quantification. These drawbacks include the interference caused by surrounding conditions such as ambient light conditions, shooting distance and imaging angle. In addition, inter-phone operability is also another factor caused by camera optics and smartphone proprietary software for image processing. Even though custom-designed 3D printed accessories compatible with different types of smartphones have been proposed,[16,23,24] these accessories can only eliminate ambient light interference. In another study, a scene-specific calibration method was proposed to use raw images for scientific data acquisition.[25] The raw image is an unprocessed image and offers linear intensity values with scene radiance regardless of proprietary software of the smartphone and image formats. The problem of inter-phone repeatability for the colorimetric analysis has been addressed employing a calibration curve created based on sensor type, target analytes, units of concentration and reference data points.[26] The calibration approach was also employed[27] aiming to compensate for ambient lighting conditions, imaging distance/angle and smartphone brand. The color calibration was implemented in two steps. First, all sensor units were calibrated using four spots to align the same black and white backgrounds, then sensors were corrected individually using two spots. Zhang *et al.*[28] proposed a color calibration for a lens-based imaging system using a color checker as the ground truth of color intensities. The color cali-

bration was based on polynomial regression and the images were processed with image normalization and white balance, correction of lightness, correction of desaturation, and color transformation steps for accurate calibration. As an alternative to color calibration, artificial intelligence-based approaches gain relevance due to their powerful utilities such as automated decision-making and self-learning from the image. Machine learning classifiers were trained with a dataset containing images from four different smartphones under seven different illumination conditions to ensure inter-phone repeatability under versatile illumination.[17] In another study, colorimetric analysis of glucose was performed with deep learning methods to ensure the robustness of the system against illumination variation and smartphone brands.[29]

The focus of this review is to explore smartphone-based colorimetric glucose monitoring techniques. Colorimetric methods and advanced techniques where the studies involve the keywords 'smartphone' and 'glucose' were included based on their appearance in a WOS database search. The review covers recent advances and developments in diagnostic and management technologies for diabetics and how such advances enhance the performance of smartphone-based diagnostic and management systems. Progress in data collection, transferring and analyzing, non-invasive/invasive glucose detection, bioanalytes and nanostructures for glucose detection in various body fluids, designs for multiple analyses including 3D-printed materials, screen-printed electrodes, and polymeric templates is covered. Finally, directions for future studies including open research challenges are provided for smartphone-based platforms.

2. The importance of glucose monitoring

Self-monitoring of blood glucose (SMBG) with smartphone technologies (and associated connectivity with other devices) enables easy monitoring for diabetic individuals, diminishing patient compliance related issues and reducing related complications.[30] It is useful to empower patients to manage/control their diabetes, highlighting the importance of manufacturing simple user-friendly technology to aid the growing number of patients worldwide. Patient education is also important to ensure they are knowledgeable about diabetes enabling them to adjust their diet, exercise, medication, *etc*.[31] Smartphone applications for physical activities such as step counts, calorie expenditure, heart rate information, *etc*., facilitate patients to control these variables. DiaBits and T1 Exercise applications were developed for Type 1, while Glucose buddy, One Drop diabetes management, mySugr, and GlucoseZone were developed for both Type 1 and Type 2.[32] Moreover, the applications are classified into three categories in Google Play Store and Apple App Store; glucose monitoring applications, carbohydrate counter mobile applications, and exercise and diabetes mobile applications for Type 1 diabetes.[30] A multi-national online survey[33] was conducted to investigate the role of continuous glucose monitoring (CGM), diabetes applications and self-care behavior in Type 1 and Type 2 diabetes. The results show that CGM technologies reduce the likelihood of experiencing hyperglycemia and hypoglycemia in Type 1 diabetes. It is important to note that the likelihood of experiencing hyperglycemia in Type 2 diabetes has been reduced significantly when using smartphone diabetes applications.[34]

By the year 2020, 222 Android and 123 iOS diabetes-related applications had been released with English interfaces which are categorized in Fig. 3 based on their functionality. The applications capable of monitoring the glucose level and converting from mmol L^{-1} to mg dL^{-1} are classified as management. The informative ones include various nutrition, diet, and exercise advice and aim to raise awareness about Type 1, Type 2, and gestational diabetes by sharing informative articles with the user. Some of the applications have both management and informative features which are classified as multitasking. Finally, we defined the applications as supportive where patients are followed-up online by doctors and on the forum platforms where diabetic patients share their experiences. Education carries great importance in controlling the course of diabetes. For this reason, it is necessary to identify and eliminate the factors that restrict patients. To overcome these restrictions, personalized feedback support and recommendations suggest that patients act according to the rhythm of the disease and benefit more from the advantages of the smartphones.[35] Although glucose monitoring is mostly performed with point-of-care self-monitoring devices such as glucometers, painless and non-invasive techniques based on colorimetric methods have been developed for biosensors in recent years. With the latest advances in smartphone technology, the internal camera provides adequate information for colorimetric analysis.[36] The smartphone cameras were used as

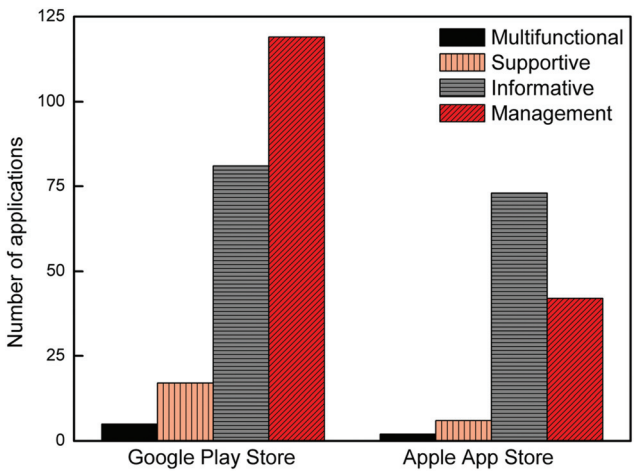

Fig. 3 The number of diabetes-related applications available for Android and iOS based smartphones found after a search conducted in the Google Play Store and the Apple App Store, respectively, in the year 2020. The apps have been classified based on their functionality as either multifunctional, supportive, informative, or management.

RGB (Red, Green, Blue) sensors for colorimetric determinations of different analytes.[23,24,37–41]

The commercial Accu-Chek active visual test strips have been used to develop a smartphone application by converting the RGB values to LAB (Lightness, Green-Red, Blue-Yellow) and HSV (hue, saturation, value) values.[42] The commercial test strips where visual color analysis is required have also been used in urinary glucose analysis.[27,43] The blue color was used for the quantitative analysis of the HRP–H_2O_2–TMB (3,3′,5,5′-tetramethylbenzidine) enzymatic system with a broad linear response.[43] Self-monitoring solutions offer an alternative to naked-eye glucose determination for the people who have visual problems by allowing smartphone image analysis.

3. Data collection, transfer and analysis

The network systems for smartphone-based diagnosis and monitoring tend to be based on body area networks (BANs) and personal area networks (PANs). BANs support wireless communication of wearable computing devices while PANs allow a wider network for data transmission among devices including smartphones, cloud systems and computers.[45] Communication in PANs can be wired (using USB and FireWire), or wireless using infrared, ZigBee, Bluetooth, UWB (ultrawideband), WiFi, NFC (near field communication) and GPS (Global Positioning System).

Infrared is a mobile communication technology for short ranges. It is a common, low-cost and easy to use wireless technology. The drawbacks of infrared are short transmission range, inability to penetrate walls and line of sight requirements. ZigBee is a computer networking protocol for short-range communication with low-power consumption. It is built on the IEEE 802.15.4 standard with the capability of the data rate of 40 kb s^{-1} in the 900 MHz band and 250 kb s^{-1} in the 2.4 GHz band. Bluetooth is another protocol for short-range and low-power communications operating only in the 2.4 GHz unlicensed band with 3 Mb s^{-1} data rates. UWB is a short-range and high-bandwidth communications radio technology operating in the 3.1–10.6 GHz band. The advantage of operating in this wide band is not to create harmful interference for the users in the same band. WiFi offers wireless high-speed internet and network connections based on the IEEE 802.11 standard protocol using radio waves. Common bands used in WiFi are 2.4 GHz and 5 GHz including multiple channels to be shared between networks. NFC is a short-range high-frequency wireless communication protocol for data exchange between two electronic devices over a distance of 10 cm. NFC has advantages, as compared with the aforementioned communication protocols, because of its shorter set-up time and a higher degree of security due to its shorter range. GPS is a satellite-based navigation system that uses messages broadcasted from space to calculate the exact position of an object in the area. These messages contain the current position, orbit and exact time of each GPS satellite. A GPS receiver collects messages of at least three satellites to determine the receiver location.[46]

The data obtained from the sensors need to be transmitted to a smartphone for analysis, detection, monitoring and diagnosis, resulting in rapid, low-cost and efficient treatment. Recent advances in smartphone technologies together with the increasing capability in wireless systems have led to the emergence of higher capacity networks such as WWAN (wireless wide area network) and WLAN (wireless local area network). WWAN is a standard communication network for a wide area while the WLAN offers a standard communication network over a narrow area.[47,48]

Smartphone-based wireless diagnostics and treatment platforms offer many types of tools for diabetics including continuous monitoring systems.[58,59] A set of wearable sensors were used to monitor patients with a wireless connection to a smartphone.[58] The custom-design smartphone application collects data *via* Bluetooth and compresses to speed up the transfer process to the server *via* the internet network where the data are stored and processed. An intelligent internet of things (IoT) systems is proposed to monitor diabetic patients remotely using a smartphone.[59] The level of glucose in the blood and body temperature are measured with wearable sensors, which are connected to the smartphone *via* Bluetooth. The collected data in the smartphone are transmitted to the server using the 4G network for further processing and classification. Similarly, an Android application was developed to receive the systolic and diastolic blood pressure and heart rate values from a sensor *via* Bluetooth.[60] These values can be transmitted *via* the internet of things and the patient could be alerted in case the values are outside the ordinary range. NFC link and RF antenna were used for communication between the smartphone and microcontroller-based sensor. A diabetes management system was proposed in ref. 61 including a mobile application, automated text-messaging feedback and a clinician portal, wherein a glucose meter was used to measure the blood glucose level of the patients. The data were transferred to the mobile app *via* Bluetooth, after which the mobile app transferred the data to the clinician portal *via* the internet for further analysis. An ultrasensitive optical transducer was used for wireless glucose monitoring *via* a smartphone, where luminescence images captured by a smartphone camera and transducer were processed to enable euglycaemia and hyperglycaemia discrimination. Polymer dots have been combined with Pd-porphyrin-based transducers for fluorescence imaging and PD4Gx (Pd(II) mesotetra (pentafluorophenyl) porphine (PdTFPP, D4) has been used to detect glucose by combining with GOx, due to its sensitivity and photostability, Fig. 4.[44]

Besides the aforementioned studies, there are also many commercial smartphone dependent glucose meters including Dario by LabStyle,[62] Gmates SMART by Philosys,[63] iBG Star by Sanofi Aventis and AgaMatrix. They all need to be plugged into a smartphone to benefit from the battery, memory and interface features. In addition, they can reach a cloud system using a smartphone as a data connection point. We should note that there are other invasive, minimally invasive and non-invasive glucose meters, however, exploring other glucose meters that are not smartphone-based and without wireless communi-

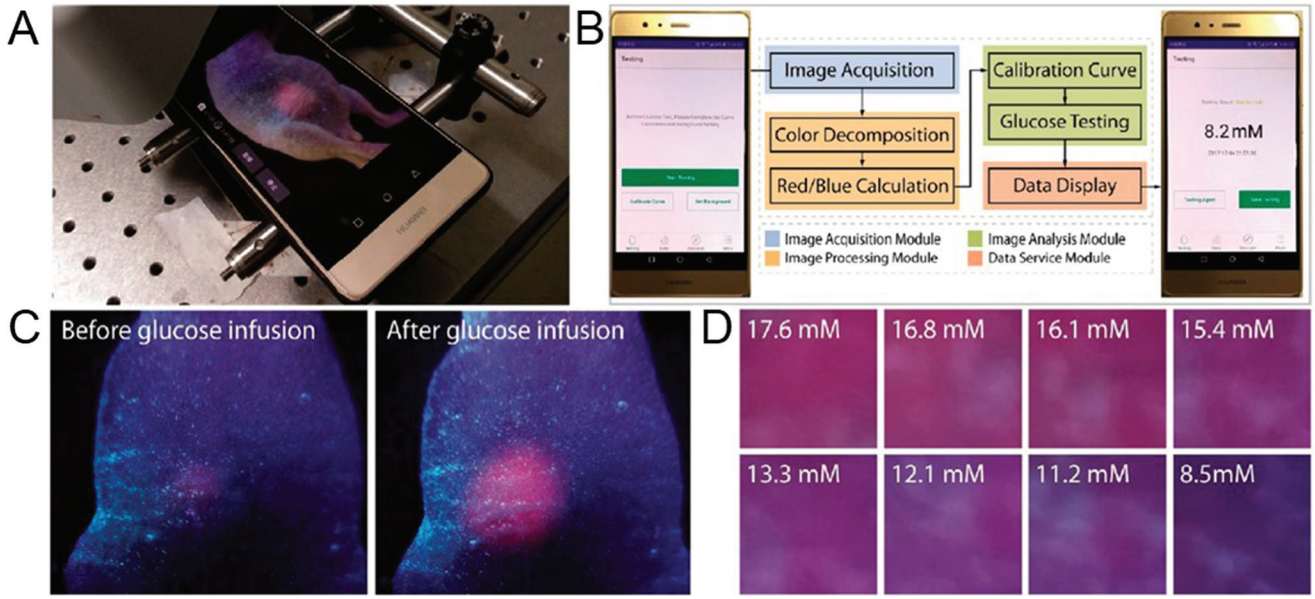

Fig. 4 *In vivo* continuous glucose monitoring in live mice using Pd-porphyrin-based transducers (PD4Gx) and a smartphone. (A) Photograph of glucose measurement in live mice. (B) Image decomposition method. The images displayed on the smartphone show the testing home page (left) and the real-time data display page (right) of the application. (C) Representative true-color photographs of the implanted PD4Gx transducer before and after glucose administration. (D) Magnified regions in the images taken by a smartphone camera at different blood glucose levels. Reproduced from ref. 44, Copyright 2018 with permission from American Chemical Society.

cation is outside the scope of this review. The reader is referred to other excellent literature for details of such glucose meters.[64,65]

4. Non-invasive and minimally invasive glucose detection

Non-invasive and minimally invasive methods for transdermal glucose monitoring are under development. These methods are based on the extraction of fluid across the barrier *via* the use of microneedles or the interaction of electromagnetic radiation with tissue such as optical detection. Different non-invasive approaches including light/fluorescence absorption, ultrasound/sonophoresis/iontophoresis, polarimetry, heat/thermal emission, photoacoustic detection, infrared, Raman/bioimpedance spectroscopy, and electromagnetic/electrochemical methods have been developed to overcome the challenges associated with invasive approaches.[65,67–69] The most recent studies with these methods are presented in Table 1, which gives a brief summary of their performance. Since many studies, focusing on these methods, require sophisticated instruments, this section includes non-invasive studies that can provide smartphone-based colorimetric glucose monitoring based on biological fluids, which are ideally combined with wearable platforms, such as sweat, tears, urine, saliva, and interstitial body fluids. The body fluids have important information about the glucose level as well as proteins, hormones, ions, and other molecules in the human body.[70] As an alternative to painful invasive methods such as a finger-prick blood test, smartphone-based non-invasive glucose detection in the body fluids potentially allows low-cost, fast, reliable, effortless measurement as a new medical control approach for diabetic patients. Tables 2 and 3 summarize the smartphone-based colorimetric glucose detection in body fluids. There are many applications based on the color change for Android and Apple devices used for personalized glucose monitoring including Color Picker, Color Name, Color Grab, UrineAnalysis, ColorAssist, and ColorLab. The preliminary studies were performed using synthetic glucose solutions and samples from food and pharmaceuticals due to the ethical issues with human glucose. Besides, they are needed to demonstrate the validity of the method for handheld analysis in various fields. The lowest LOD for glucose detection was found to be 0.21 μM using a Co_3O_4–CeO_2 nanosheet integrated paper-based analytical device.[71] The peroxidase-like property of Co_3O_4–CeO_2 nanocomposites was combined with PADs, which have the advantages of easy preparation, portability, and high efficiency, to develop convenient and sensitive colorimetric sensors for glucose detection.

4.1. Sweat

Sweat has a direct correlation with the blood glucose level enabling the use of wearable and flexible devices without equipment for analyte storage.[72,73] The determination of glucose levels is a challenging task as several distinctive issues influence the determination process such as containing sugar at a lower concentration than blood, difficulties in collecting it in a sufficient amount, and lactic acid in sweat.[72,74] Therefore, the design to be developed for the determination of glucose

Table 1 Comparison of non-invasive or minimally invasive glucose detection methods

Technique	Sample	Functional reagent	R^2	LOQ	LOD	Ref.
Optical coherence tomography	Blood glucose	—	0.91	5.0 mM l^{-1}–15.9 mM l^{-1}	5.78% mM^{-1}	49
Fluorescence spectroscopy	Glucose solutions	Boronic acid functionalized carbon nanoparticles (CNPs)	0.98	50–2000 μM	10 mM	50
Near-infrared fluorescence spectroscopy	Glucose solutions	$CuInS_2$ quantum dots (QDs)	0.99	0.005–8 mM	1.2 mM	51
Raman spectroscopy	Saliva	AuNPs onto Cu-tetra(4-carboxyphenyl)porphyrin chloride (Fe(III))	0.99	0.16–8 mM	3.9 μM	52
Surface plasmon resonance and polarimetry	Glucose solutions	—	0.99	0–500 mg dL^{-1}	10 mg dL^{-1}	53
Reverse iontophoresis	Glucose solutions	Glucose oxidase/chitosan/carbon nanotube solution	—	0–100 μM.	2.1 nA μM^{-1}	54
Mid-infrared photoacoustic spectroscopy	Photoacoustic images of the skin	—	—	0–300 mg dL^{-1}	—	55
Terahertz	Blood glucose	—	—	89.9–178.0 mg dL^{-1}	—	56
Microwave	Glucose solutions	—	—	40–140 mg dL^{-1}	0.94 MHz mg^{-1} dL^{-1}	57

from sweat should be a wearable patch type or disposable strips with multiple channels to address the issue of sufficient amount of sweat collection. Zhang *et al.* proposed a platform with a novel design of channels/patterns on filter paper for sweat collection. The success of the platform lies in intensifying the concentration of the sweat content by air-drying and, using quinone as a colorant. The glucose concentration of sweat was determined to be in the range of 50–300 μM from the photos of wet and air-dried patches captured by a smartphone.[75] The obtained range makes it possible to determine a high glucose level by exceeding the normal range of glucose in human sweat which is 50–120 μM.[74] However, it was reported in ref. 76 that the characteristic difference between blood and sweat, the need for repeated calibration of the designed device, and contact dermatitis are disadvantages of the patch type sweat sensors. Rönnemaa *et al.* highlighted the consideration of the relationship between temperature and blood sugar due to metabolic rate changes of patients exercising in a warm environment.[77] A thermo-responsive textile/paper-based microfluidic sensing system was incorporated under the collar of a shirt to detect human sweat glucose (Fig. 5A). The glucose determination was performed using three volunteers working in a high-temperature environment (~59 °C). This system was also tested enzymatically on artificial sweat where the limit of detection (LOD) was 13.49 μM. The images taken by the smartphone were split to R, G, B channels and it was determined that the noticeable change was in the R channel (Fig. 5B and C).[66] Similarly, the R channel was selected due to its higher contribution to the color change, which was the result of an enzymatic reaction, compared to the G and B channels. The proposed thread/paper-based microfluidic device possessed a LOD of 35 μM.[78]

4.2. Tears

Compared to sweat, tears contain a large number of different biomarkers, *e.g.* proteins, lipids, peptides, enzymes, and salts. These biomarkers diffused directly from the blood making the concentration more closely correlated, and due to the blood–tear barriers, tears are less complex than blood.[80] Tear glucose levels in normal people are in the range of 0 to 3.6 mM (ref. 81) while for diabetics the level is 4.7 mM.[82,83] Determining the level of glucose from tears provides a painless approach and tears can be used directly without any pretreatment, and can also be used for continuous diabetes management through practical smartphone applications. Wang *et al.* reported chitosan modified paper-based sensors for better color strength and immobilization of reagents.[84] It was reported that gray values were more sensitive to quantitative correlation between the concentrations and color variations which led them to convert RGB images to gray images. In such paper-based sensors, the LOD was 0.014 mM, and the determination of glucose from the tears of 3 healthy patients was successfully performed. As a very practical method for collecting tear samples without contamination, microchannel shaped cavities were created in contact lenses by using laser ablation (Fig. 6A). The glucose determination was conducted *via* the enzymatic reaction shown in Fig. 6B and the absorbance spectrum (Fig. 6C) was obtained for certain glucose concentrations from the calibration curve (LOD of 1.84 mmol L^{-1}). The color of the modified contact lenses can be captured *via* a smartphone camera (Fig. 6D) which contains the reference data for the colorimetric analysis. Fig. 6E shows the optical density trend at 670 nm with a second-order polynomial fitting (R^2 = 0.99). The nearest neighbor method was used to determine the glucose level and the RGB values, shown in Fig. 6F, were obtained from the glucose assays.[79]

4.3. Urine

Urine is another diagnostic body fluid that can be readily and noninvasively collected. The normal glucose levels in urine for a healthy adult range from 2.78–5.55 mM.[85] Glucose screening using urine is a simple method which indicates a high glucose

Table 2 Summary of imaging methods and detection software for glucose detection

Sample	Imaging	Processing software/detection device	Ref.
Serum/urine	Canon PowerShot S5 IS digital camera/iPhone 4.0	Image J/Objective C for application/development HSV color space-μPAD	121
Glucose solutions/glucose drink	Smartphone	Image J/Gray color value-Filter paper	115
Glucose solutions/human serum	Smartphone	Color Picker Application-PADs	71
Glucose solutions	iPod Touch	Image J-3D printed device including cuvette chamber, slots for diffused filters and chambers for LED light sources.	122
Artificial sweat/human sweat	Smartphone	Image J/Lab value-polydimethylsiloxane (PDMS) microfluidic device	75
Artificial sweat/human sweat	Smartphone	'Color Name' smartphone based software-PU textile based microfluidic device	66
Artificial sweat/human sweat	Smartphone	'Color Grab' application software/RGB values – μTPAD	78
Glucose solutions/human serum/human tear	Smartphone (iPhone 6)	Image J/Gray value-multilayer-modified paper-based sensing platform	84
Glucose solutions/artificial urine	Smartphone	UrineAnalysis Android-application/RGB values-paper-plastic hybrid microfluidic lab-on-a-chip	86
Glucose solutions/artificial saliva	Smartphone (iPhone 7)	RGB values/MATLAB/Xcode 8.0 for application development- μPADs	94
Blood glucose	Smartphone (iPhone 5s)	'ColorAssist' application/RGB values-designed integrated blood glucose detection device (IBGDD) including a cover and baseplate set, a disposable lancet, and a light guide channel.	105
Whole blood/glucose solutions	Sony DSC-HX300 digital camera, Samsung Galaxy S5 smartphone, Samsung Galaxy Tab A Tablet Motorola Moto G4 Play smartphone	Image J/Avidemux 2.6/The Anaconda distribution of Python (Continuum Analytics), OpenCV (Open Source Computer Vision), and Android Studio (Google) for development – μTPAD	106
Glucose solutions	Smartphone (Xiaomi MI 2SC)	Image J-Paper-based bipolar electrode-electrochemiluminescence (BPE-ECL) device	123
Glucose solutions/blood glucose	Scanner(Epson Perfection V700), microscope (USB-embedded handheld digital microscope), and the smartphone (LG Optimus Vu).	Photoshop software (Adobe Systems) – Paper-based 3D microfluidic chips	124
Glucose solutions/real samples (food and pharmaceutical)	Smartphone	'ColorLab' application/HSV data-multiplexed colorimetric enzymatic biosensors based on poly(ANI-*co*-AA) composite film	125
Glucose solutions/human serum	Smartphone (LG Optimus L5 II)	Image J/RGB colors-Multi-well microplate	126
Glucose solutions	Smartphone (LG G2)	Image J/RGB colors/Microsoft PowerPoint 2016-optical-signal-transducing	127
Glucose solutions	Smartphone	Image J/Gray value-embossed-paper devices	128
Glucose solutions/human serum	Smartphone (iPhone 6)	Image J/Adobe Photoshop/Gray value- μPAD	129
Glucose solutions/human serum	Smartphone (I8000U, Samsung) A CCD Camera(HDF70-A, Hongjia Optical Display Technology)	Adobe Photoshop CS4/RGB colors-multiplex analysis fan-shaped microfluidics	130
Glucose solution/real samples	Smartphones (iPhone 5S and Samsung J5) Scanner (Canon i-sensys MF4780dn)	$L^*a^*b^*$ color space/'C-Measure Lite' application/'Color Grab' application/' 'DigitalColor Meter'/RGB colors-paper based sensing	131
Glucose solution	Smartphones (HTC sensation XE, iPhone 5s, and Nokia Lumia 920)	Cell Phone Spectrometer Application	132
Glucose solution/urine	Smartphones (iPhone 4, Samsung Galaxy S II or MEIZU MX2)	Cam Card, Adobe Photoshop/RGB colors-wax-based filter paper	27
Serum samples	Smartphone (iPhone 4)	ColorAssist application/RGB colors-commercial test slides	133
Serum samples	Smartphone	Image J-μPAD	134
Artificial urine	Smartphones (iPhone 5 and Samsung I5500 Galaxy 5)	RGB colors-colorimetric urine test strip (cobas® Combur3 Test®, Roche)	26
Glucose solutions	Smartphone	Color detector application/RGB colors	135
Glucose solutions/human serum	Smartphone	HSV Application/RGB-HSV values	136
Urine glucose	Smartphone (MIX6X Xiaomi)	Color Picker 1.5.2 Application/RGB colors	43

level when the concentration of glucose is above 5.55 mM.[85] In a urinary system, H_2O_2 causes a color change in the solution which provides a colorimetric analysis of glucose. TMB has been used in ref. 43 that is oxidized as a blue product by H_2O_2 to observe changes in the color. The inverse ratio between the intensity values of RGB and glucose concentrations offers a new methodology that can be implemented with a smartphone camera. Urine test strips cause deviation in measurements

Table 3 Summary of indicator, limit of quantification (LOQ) and LOD values for glucose detection

Sample	Indicator	LOQ	LOD	Ref.
Serum/urine	MOF/TMB	Up to 150 μM	2.5 μM	121
Glucose solutions/glucose drink	Antimony-doped tin oxide nanoparticles/TMB	0.5–80 mM	21 μM	115
Glucose solutions/human serum	Co_3O_4–CeO_2/TMB	0.005–1.5 mM	0.21 μM	71
Glucose solutions	AgNPrs	20–100 μM	19.8 μM	122
Artificial sweat/human sweat	4-Aminoantipyrine (AAP)/sodium 3,5-dichloro-2-hydroxybenzene sulfonate (DHBS), HRP	50–300 μM	50 μM	75
Artificial sweat/human sweat	HRP/TMB	50–600 μM	13.49 μM	66
Artificial sweat/human sweat	HRP/TMB	50–250 μM	35 μM	78
Glucose solutions/human serum/human tear	HRP/TMB	0.02–4.0 mM	14 μM	84
Glucose solutions/artificial urine	—	0–19.42 mM	—	86
Glucose solutions/artificial saliva	HRP/TMB	0–1 mM	0.02 mM	94
Blood glucose	—	2.775–27.75 mM	—	105
Whole blood/glucose solutions	HRP/TMB	—	48 μM/12 μM	106
Glucose solutions	Luminol	0–5 mM	17 μM in PBS/30 μM in artificial urine	123
Glucose solutions/blood glucose	Tetrabromophenol blue (TBPB), HRP, Methylene Blue water-soluble dye, Congo Red water-soluble dye	0–50 mM	—	124
Glucose solutions/real samples (food and pharmaceutical)	HRP/tyrosinase	25–200 μM	109 μM	125
Glucose solutions/human serum	HRP/TMB	0.333–4.884 mM	0.100 mM	126
Glucose solutions	HRP/4-AAP/*N*-Ethyl-*N*-(2-hydroxy-3-sulfopropyl)-3,5-dimethylaniline (MAOS)	0–10 mM	—	127
Glucose solutions	HRP/*o*-Dianisidine	0–0.444 mM	—	128
Glucose solutions/human serum	4-AAP/DHBS/TOPS	0.01–10.0 mM	3 μM	129
Glucose solutions/human serum	DHBS/Peroxidase	3.0–8.0 mM	—	130
Glucose solution/real samples	4-AA	Up to 10 mM	0.38 mM	131
Glucose solution	ABTS, HRP, AuNPs	0.8–20 mM	0.2 mM	132
Glucose solution/urine	Bromocresol purple, bromocresol green, bromocresol blue, chromophenol red	—	—	27
Serum samples	4-Aminoantipyrene 1,7-dihydroxynapthalene	1.665–18.58 mM	—	133
Serum samples	HRP	5–17 mM.	0.3 mM	134
Artificial urine	Peroxidase	0–16.65 mM	5.106 mM (Android) –3.830 mM (iOS)	26
Glucose solutions	Ti_3C_2/TMB	0.01 mM–0.32 mM	8.82 μM	135
Glucose solutions/human serum	HRP, TMB entrapped within zeolite imidazolate framework (ZIF 8)	100–3000 μM	250 μM	136
Urine glucose	HRP/TMB	0.22–55.5 mM	—	43

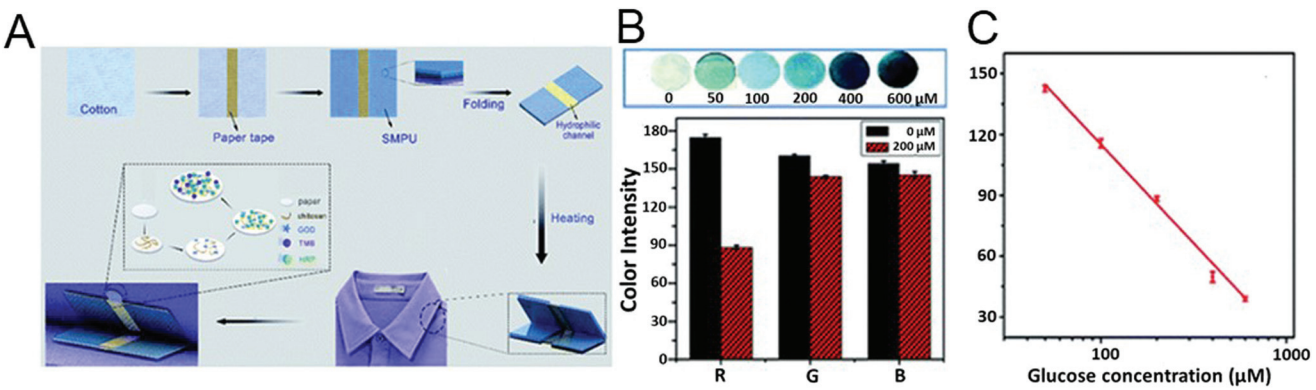

Fig. 5 (A) Fabrication of the thermo-responsive textile/paper-based microfluidic sensing system. (B) Images of the paper-based colorimetric sensors obtained after testing a series of artificial sweat samples containing different glucose concentrations. Bottom; the R, G and B values of the artificial sweat samples spiked with 0 and 200 μM glucose; and (C) plot of the R values against the logarithm of glucose concentrations. Reproduced from ref. 66, Copyright 2019 with permission from Royal Society of Chemistry.

over time as the volume cannot be controlled when the strip is dipped into urine. Therefore, the efficiency of these urine test strips was improved by including a PDMS pump, providing volume control, with a single-channel integrated into a microfluidic lab-on-a-chip (LOC). To test the system, URiSCAN test strips were embedded into the disposable paper-plastic micro-

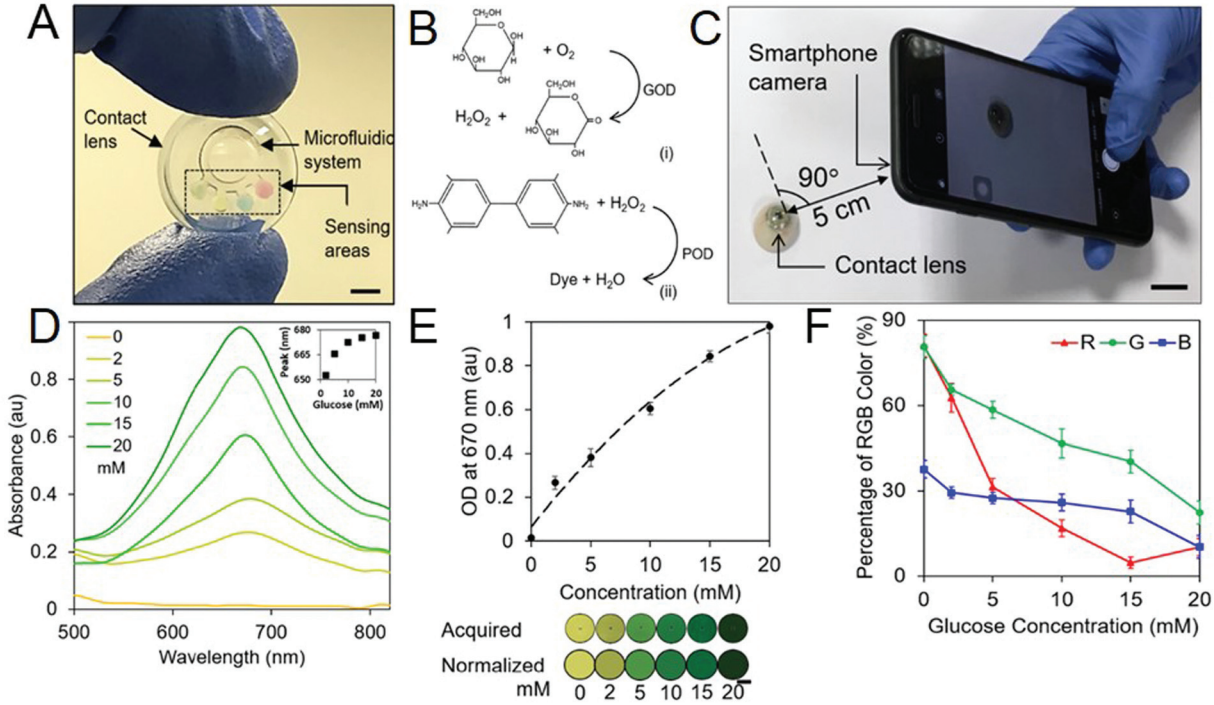

Fig. 6 (A) Photo of the microfluidic contact lens sensing platform. Scale bar: 5.0 mm. (B) Working principle of the glucose biosensor. β-D-Glucose reacts with oxygen producing hydrogen peroxide (i), which oxidizes 3,3′,5,5′-tetramethylbenzidin (ii). (C)The color change of the sensors is imaged using a smartphone camera (D) Absorption spectrum of solutions at glucose concentration of 0.0, 2.0, 5.0, 10.0, 15.0, 20.0 mmol L^{-1}. The inset shows the calibration curve. (E) Optical density trend of tear glucose sensors at 670 nm. The image of color changes shows the acquired (first row) and normalized (second row) colors imaged in solutions having different glucose concentrations. (F) RGB characterization of glucose sensors. Reproduced from ref. 79, Copyright 2020 with permission from Elsevier.

chip to detect glucose as well as protein, pH, and RBC of blood, using 40 μL of urine as shown in Fig. 7A. When the dipstick method was compared with the developed LOC platform in Fig. 7B, the change in the hue value for the LOC was smaller during the reaction time. Therefore, the reaction time had less impact on the LOC device which can perform repeatable measurements with high accuracy. Hue values were calculated from the RGB values of the images to determine the colorimetric change with a smartphone camera. The values had been used in the Android-based 'UrineAnalysis' application, as shown in Fig. 7C.[86]

Wang *et al.*[87] used an ambient light sensor (ALS) instead of a smartphone camera due to its drawbacks such as smartphone brand, capturing distance, and illumination. A quantitative urine sugar analysis was performed using a smartphone with ALS, based on the color-fading from deep blue to light blue, resulting in the formation of H_2O_2 color in the HRP–H_2O_2–TMB system. This proposed method is low-cost and offers high accuracy for a rapid/rough screening of urine glucose of diabetic patients.

4.4. Saliva

Salivary glucose detection is interesting due to the ease of collection in a painless fashion, good correlation between saliva and the blood glucose level,[88] and excellent selectivity against dopamine and cortisol.[89] Besides, low-cost systems with high sensitivity have been developed by using paper microfluidic devices and non-enzymatic methods for glucose determinations in saliva.[90,91] The glucose level can be measured in saliva using colorimetric methods due to a linear response between 43 pM and 220 μM, with a detection limit of 1 pM.[92] It is worth mentioning that the normal glucose concentration is in the range of 27.75–55.50 μM in human saliva.[93] For the enzymatic determination of glucose in saliva, a portable, smartphone-based colorimetric glucose determination method with a LOD of 0.02 mM has been obtained by modifying the disposable paper with graphene-oxide. An iOS-based application was developed to calculate glucose concentrations based on the calibration curve constructed with the calculation of the generalized pixel value using R, G, B channels of each pixel within the region of interest.[94] In a pioneering work, the effects of possible chemical interferences such as the presence of ascorbic acid, lactic acid, and lactose in the mouth (*i.e.* pH of the saliva), and systematical variables such as the location of the smartphone camera and illumination on the biosensor response were reported.[95] Considering the disadvantages of the reported non-invasive sensors in terms of the usability, portability, and accuracy of the device, they developed a more user-friendly smartphone-based biosensor capable of determining glucose in saliva samples without a dedicated device. The sensor was easily fabricated by the immobilization of GOx along with a pH indicator on a paper-based strip. The sensi-

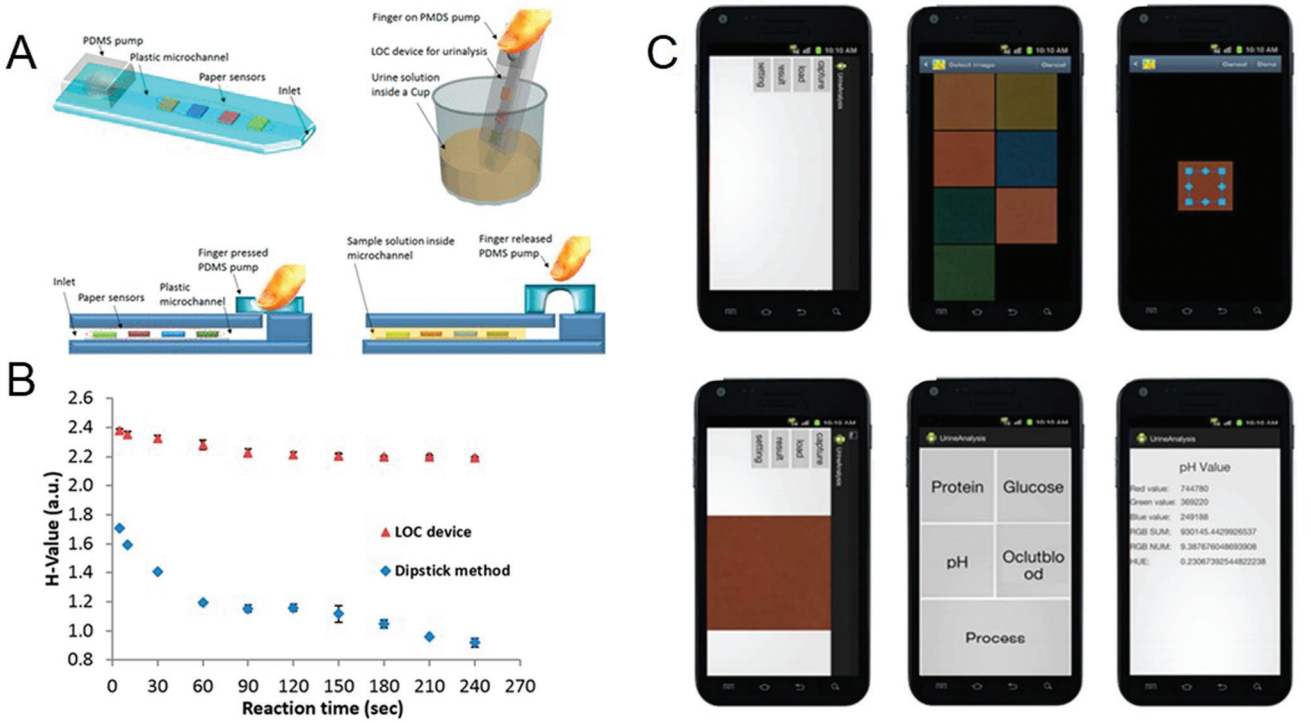

Fig. 7 (A) Top left; conceptual scheme of a hybrid lab-on-a-chip (LOC) device made of patterned polycarbonate sheet for urinalysis, top right; urine solution inside a cup, and its operational steps, bottom left; finger force is applied to initiate negative pressure to move sample solution into the LOC device chamber, and bottom right; the solution flows into the device chamber to react with the reagent. (B) Measurement of hue value by the reaction time of the reagent strip in urine solution using both the dipstick method and the developed LOC device. (C) Screenshots of the developed 'UrineAnalysis' Android application for the colorimetric test. Reproduced from ref. 86, Copyright 2017 with permission from American Chemical Society.

tivity of the sensor was increased by using bromocresol purple compared to methyl red used in a previous work.[96] The slope method was selected rather than the differential method in their smartphone application as it achieved further enhanced sensitivity and reduced ambient light interference without the requirement of baseline correction.

4.5. Interstitial body fluid

ISF contains electrolytes, lipids, glucose, enzymes, hormones, proteins and inorganic substances, and therefore exhibits similar characteristics to blood.[97,98] However, it has been observed that there is a time difference in the measurement of glucose levels between blood and interstitial body fluid because it takes time for the glucose to reach ISF *via* the blood capillary after the glucose level first changed in the blood.[76] The estimated delay was about 5–6 minutes between the blood and the ISF.[99] The glucose levels in ISF for a healthy adult are 3.9–6.6 mM, and for diabetics 1.99–22.2 mM.[85] In order to measure the glucose level using ISF, sampling has been performed either by ultrafiltration,[100] dual/reverse iontophoresis,[101,102] microfluidic chip,[103] or microneedle patches.[104] As seen in Fig. 8, subcutaneous tattooing is a way to perform the colorimetric method, which determines the glucose level in ISF. GOx, TMB, and peroxidase were used to monitor the RGB values of the color change with a smartphone, and the glucose concentration could be determined up to 50.0 mmol L^{-1} using MATLAB. Using a skin model, the biosensing ink was injected into the dermis layer, and glucose concentration was observed by the color changing from yellow to dark green under visible light, which corresponds to 2 to 50 mmol L^{-1}. In addition, the stability of the method was tested using a 5 mmol L^{-1} glucose solution. After 30 minutes under UV light, no change was observed in the absorption peak.[76]

4.6. Wearable sensors

With the onset of digitization of diabetes monitoring, wearable systems represent a convenient method for monitoring diabetes, especially Type 1 diabetes, where continuous monitoring is crucial.[107] Wearable systems in connection with smartphones allow continuous monitoring by the user, while sample collection can be performed painlessly, which is an important advantage[108] as it improves patient compliance. Sensors, that are miniaturized and/or flexible, offer ease of use.[109] Flexibility and durability are critical functions for wearable sensors. If the material used is stiff, it may affect the stabilization during the operation and cause the targeted measurement to be wrong. The sensor design should be resistant to the chemicals used, flexible, and permeable to air to support user's comfort. Wearable glucose sensors can be produced by using different materials in order to vary their

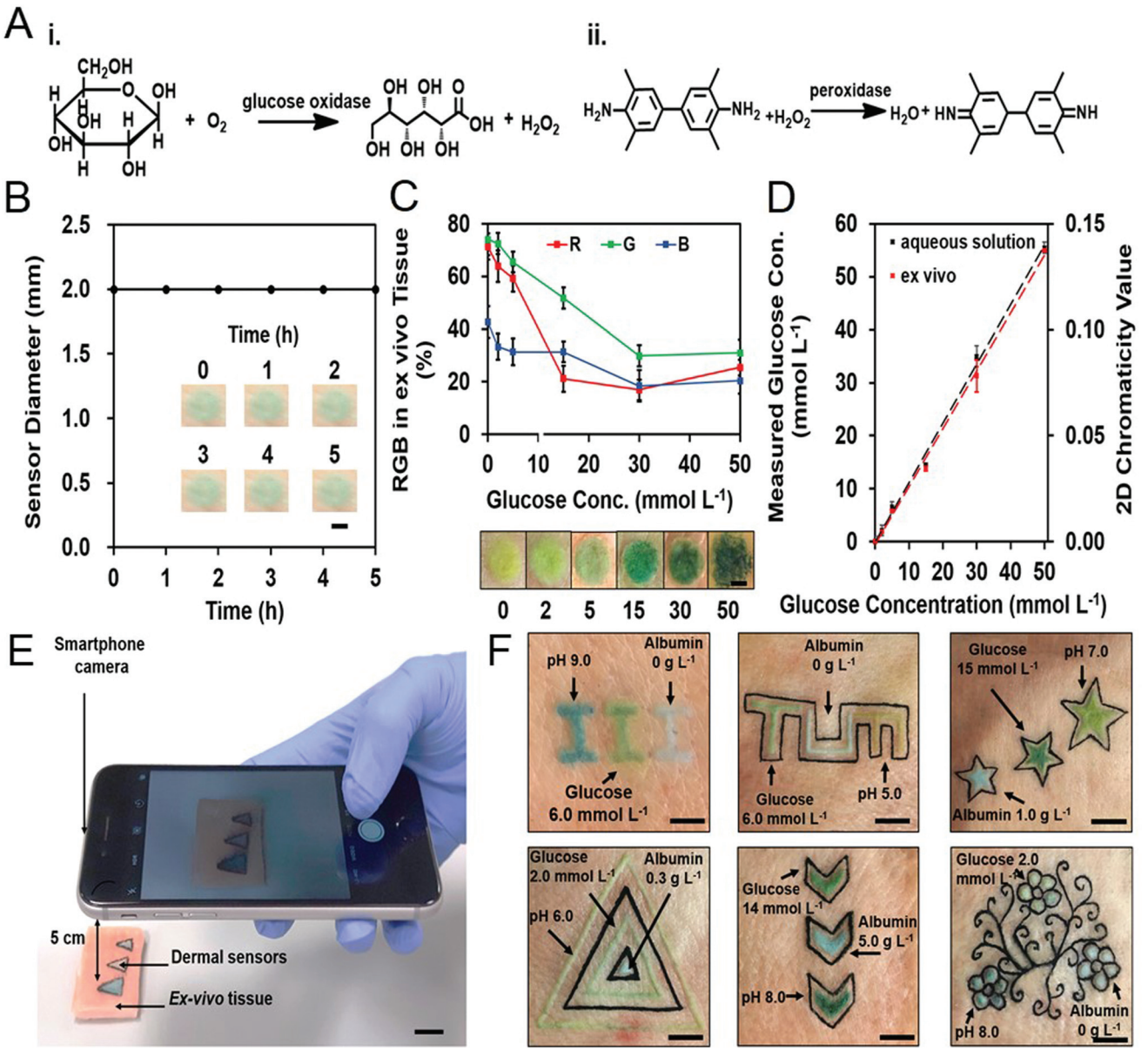

Fig. 8 Dermal glucose sensors. (A) Chemical structures of the glucose-sensing compounds (i) oxidation of D-glucose to D-gluconolactone and formation of hydrogen peroxide, (ii) Oxidation of TMB to form a blue-green dye in the presence of hydrogen peroxide, (B) diffusion test of the glucose sensor. (C) RGB triplets of dermal biosensors at different glucose concentrations (0–50 mmol L^{-1}). (D) Smartphone readouts of glucose sensors in aqueous solutions (black) and in *ex vivo* tissues (red) in response to glucose concentrations (0–50 mmol L^{-1}). (E) Smartphone camera imaging. (F) Multiplexed dermal biosensors with individual areas devoted to the sensing of a different analyte, yielding different colors based on the concentrations of pH, glucose, and albumin. Reproduced from ref. 76, Copyright 2019 with permission from Wiley-VCH.

mechanical properties. The commonly used materials for such wearable glucose sensors, *e.g.* textile fabric/cloth, polymer composites, and papers can be transformed into tattoos, patches, or contact lenses and act as sensors with integrated electronic devices.[110,111] Additionally, it is essential that the sensors are resistant to mechanical deformation and provide consistent, reliable results under stretching.[112]

Non-invasive wearable glucose sensors are capable of detecting the level of glucose from body fluids such as sweat, tear, urine, and saliva.[113,114] For instance, sweat is the preferred fluid for the development of wearable systems. Zhang *et al.* designed hydrophobic channels on filter paper using a wax printer for sweat collection.[75] Sweat diffused quickly through these channels using capillary force. A wearable glucose sensor was fabricated by the integration of the filter paper onto the medical tape which was punched for sweat inlets/outlets, Fig. 9A–C. The sensor can detect glucose concentration in the range of 50 to 300 μM with a colorant, quinone (Fig. 9D). After a workout, the patches collected from humans were imaged with a smartphone to determine sweat

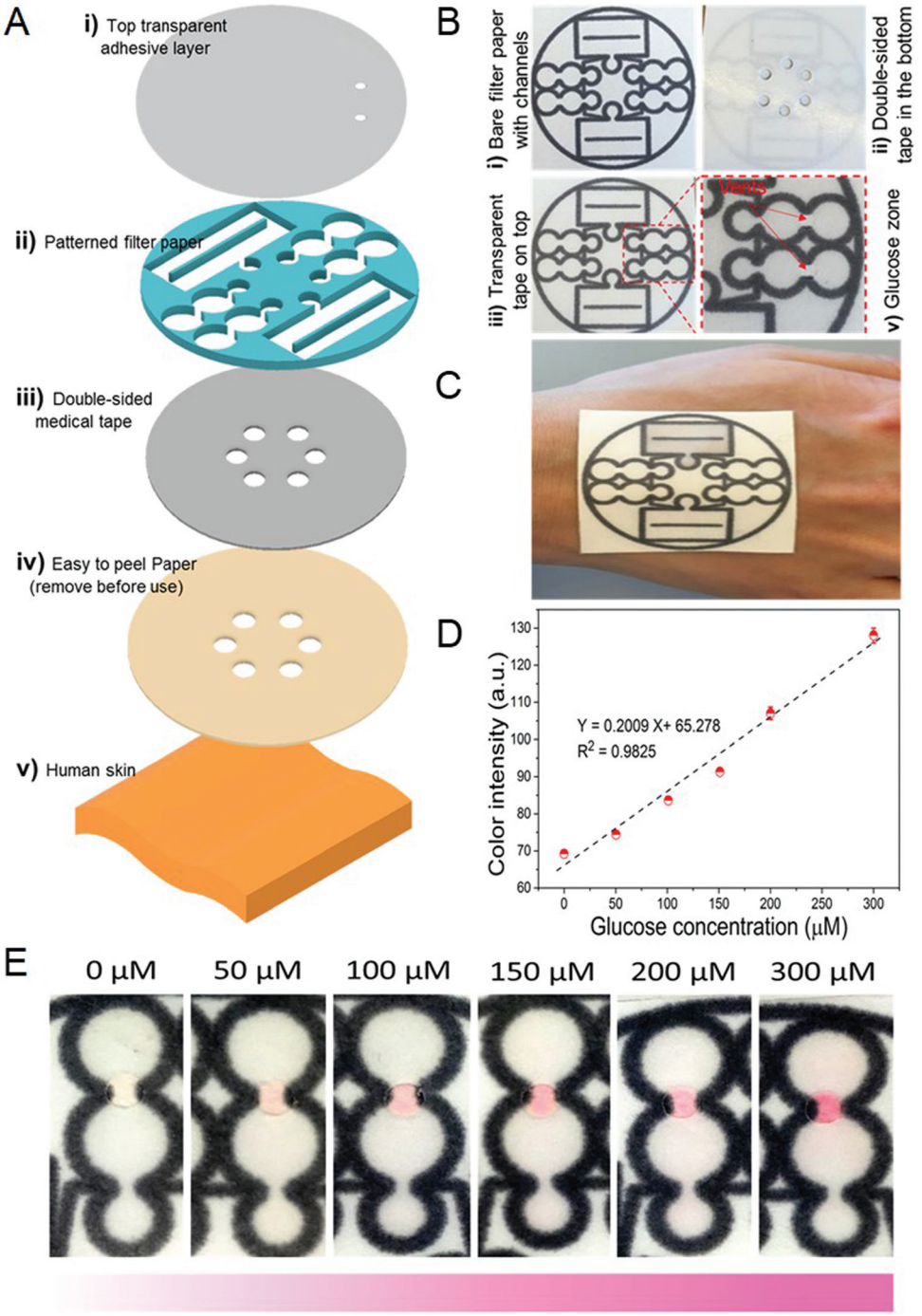

Fig. 9 Schematic design of the wearable device for sweat collection and biosensing. (A) Schematic illustration of the wearable point-of-care device layers, including the (i) top transparent adhesive layer, (ii) the pattern supported on filter paper, (iii) the double-sided medical tape, and (iv) a protective piece of paper, after being fully assembled, can serve as a patch that can be mounted on (v) human skin. (B) Images of the device before and after the addition of the transparent and medical tape layers, along with a magnified image of the glucose detection zone. (C) Image of the wearable device attached on a human hand. (D) Glucose concentration level against the color intensity. (E) The color intensity of the imaged pictures against the glucose concentration. Reproduced from ref. 75, Copyright 2019 with permission from Royal Society of Chemistry.

loss and pH levels. The color change in the air-dried patches was then re-imaged to determine the amount of glucose as seen in Fig. 9E. Microfluidic paper-based devices (μPADs) are commonly used in wearable systems for glucose determination from sweat. For this purpose, a microfluidic thread/paper-based analytical device (μTPAD) was designed as a wearable sensor and a smartphone was used to determine glucose from human sweat.[78] The designed μTPAD was composed of an

absorbent patch, a hydrophilic cotton thread, and enzyme and colorimetric reagent modified filter paper. The color change from slight yellow to blue by the enzyme-catalyzed reaction on this paper makes it possible to analyze by smartphone imaging. The sensor can detect glucose concentration in artificial sweat samples in the range from 50 to 1500 μM.

Another wearable sensor was developed by inserting it into a diaper to determine glucose level from samples of urine. The system consists of a surface module, reference color module, sampling collection module, self-locking module, and reagent pad module. The system has a self-locking system to prevent contamination from subsequent urination, and it closes after the urine enters through the sensor channel, which is attached to the diaper. Urine was analyzed by the colorimetric reaction in the reagent pad module to read the glucose level on the smartphone.[116] An image was taken using a smartphone camera from the reagent pad at least 30 minutes after the diaper was used. The R, G, B values were analyzed with MATLAB software. The test color was determined corresponding to the reference color of 50 × 50 pixels. Using the Euclidean equation, the Euclidean distance (D) was obtained from the R, G, B values from the center of the pad. Upon naked eye detection, when the D value was less than 5, the test and reference colors were reported as the same. It was also reported that RGB values were stable from 20 min to 480 min, which is a reasonable time interval for baby and elderly care. Similarly, a 'tape-in-diaper sensor' was produced, which is attached to the diaper with the help of double-sided adhesive tapes. First, the tapes were punched, and then the sensor was prepared by placing fabrics filling and indicators between the tape-layers.[117] The fabric-filled microwells were immobilized by adding a colorimetric reagent containing GOx, HRP, potassium iodide, and trehalose which was mixed with gelatin to avoid leaching. After drying, different glucose concentrations ranging from 0 to 6.0 mM were drop-cast onto the microwells. The color of the microwells was shifted from colorless to yellow with rising glucose concentration leading to an increment in R and G values and decrement in the B value. More importantly, sensitivity tests were performed using normal urine, collected from a healthy volunteer, and artificial urine spiked with abnormal targets to mimic potential diseases. Apart from phenylpyruvate, the concentration of which was low in the simulated urine samples, the amounts of glucose, nitrite, and protein were found to be high compared to the healthy urine sample. Although the sensitive detection of phenylpyruvate is difficult by colorimetry, the detection of the absence or presence of most biomarkers in urine has served as a platform for further clinical diagnosis.

Apart from body fluids, another non-invasive analyte used in wearable sensors is volatile organic compounds (VOCs) in a patient's breath as markers to detect glucose levels. Due to the correlation between ethanol and acetone concentrations, and glucose levels in breath, sensors monitoring these components have been integrated into wearable smart wristbands.[118] The lowest blood glucose level detected was 1–3 parts-per-million (ppm) and 0–20 parts-per-billion (ppb), and the high blood glucose level was 5–7 ppm and 35–50 ppb for acetone and ethanol, respectively. Two commercially available metal–oxide semiconductors have been employed as chemical sensors with different sensitivities for glucose level detection. This wearable wristband included the Arduino-based Adafruit FLORA microcontroller platform, a GPS module, a light-emitting diode (LED), and a rechargeable Li-ion battery.[118]

5. Invasive glucose detection

The most common and economically viable method for the detection of glucose levels in blood can be performed through finger-prick tests. The test strips functionalized by specific enzymes are used to obtain chemical reactions with blood glucose, and changes in the current between the test strip and the reference electrode, or changes in the color of the strips.[120] Although no additional blood glucometer in a typical colorimetric method for SMBG is needed, differences in individual color observation lead to low accuracy measurement. To overcome this problem, researchers are trying to make hardware applications such as image analysis software, a computer with a scanner or camera, and a smartphone to analyze the color value of blood glucose strips. Smartphones are ideal candidates for colorimetric detection because of their high usage rate by a wide range of age groups, and they can be combined with specifically developed applications. A portable colorimetric biosensor for self-monitoring of blood glucose was designed using an integrated glucose detection device with an automatic glucose concentration analysis software installed on a smartphone.[105] With a light-guiding channel, the light from the smartphone's liquid crystal display was reflected and guided to glucose test strips to detect color change (Fig. 10A). The analysis software was developed by using different glucose concentrations from 50 to 500 mg dL^{-1} as shown in Fig. 10B. Images of the test strip were taken by a smartphone camera and the blood sugar of 20 diabetic patients was measured with 100% accuracy. Erenas *et al.*[106] used a distinctive microfluidic design combined with thread and paper capable of detecting glucose levels from only 3 μL of whole blood (Fig. 10C–E). The device, μTPAD, has a membrane to separates red blood cells from whole blood. A smartphone, tablet, and digital camera have recorded videos which were rendered as a single frame image with Avidemux 2.6. An application was developed by the Anaconda distribution of Python, OpenCV and Android Studio. For the enzymatic determination of glucose, the LOD value was found to be 48 μM and 12 μM for 12 s and 100 s which are the required time periods for initial rate and equilibrium measurement by using the calibration function shown in Fig. 10F. The only drawback of this system was reported to be activity loss of the enzymes.

6. Bioanalytes and nanostructures for glucose detection

Due to the nature of optical methods, it is clear that there are exciting opportunities for developing new methods and hard-

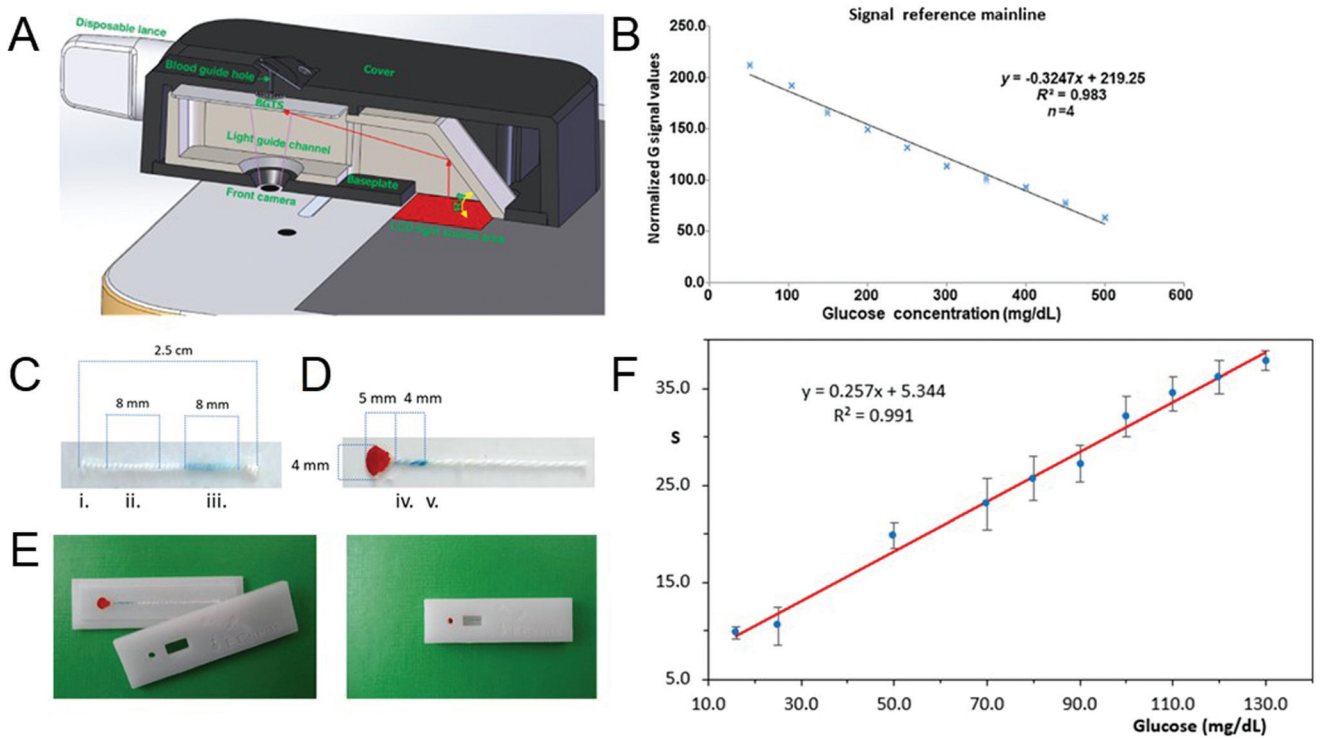

Fig. 10 (A) Smartphone and integrated blood glucose detection device, comprising the blood glucose test site, cover, baseplate, light guide channel, and disposable lancet. (B) Signal reference mainlines based on the normalized value of the G signal. Reproduced from ref. 105, Copyright 2019 with permission from SPIE Digital Library. (C) Picture of the μTAD for glucose; (i) sampling region; (ii) detection region; (iii) transduction region. (D) Picture of μTPAD for whole blood glucose: (iv) red blood cell paper-based separation membrane and sampling area; (v) detection and transduction area. (E) Case designed to contain the μTPAD with a hole for blood sampling and a window for video recording. (F) Calibration of μTPAD obtained from whole blood spiked samples using saturation (S) as an analytical parameter. Reproduced from ref. 106, Copyright 2019 with permission from Elsevier.

ware for smartphone applications.[137] The colorimetric method is the most prominent for the determination of glucose that combines camera technology and bioanalytical science with smartphones (potentially employing enzymatic or non-enzymatic colorimetric assays based on the conversion of target analytes into color changes). Colorimetric biosensors are practical, simple, and inexpensive, and can, therefore, be used for point-of-care diagnosis without any requirement for sophisticated devices. Their combination with software to convert colorimetric data to numerical output will broaden their potential use. Enzymes such as glucose oxidase (GOx), glucose dehydrogenase (GDH), hexokinase, 2,2′ azino bis(3-ethylbenzothiazoline-6 sulfonic acid) (ABTS), and horseradish peroxidase (HRP) participate in glucose level detection.[138] GOx is the most commonly used homodimeric enzyme due to its high specificity to catalyze the oxidation of glucose into gluconic acid with by-product hydrogen peroxide (H_2O_2).[139,140] Thus, the detection of glucose concentration is carried out electrochemically by determining H_2O_2 produced or O_2 consumed. A chromogen, such as TMB, forms a colored product that makes colorimetric determination possible by the catalytic oxidation of H_2O_2 with peroxidase resulting in blue coloration.

The optical property of localized surface plasmon resonance (LSPR) of metal nanoparticles is quite convenient for colorimetric detection. Colloidal silver nanoprisms (AgNPr) have been used for glucose detection enzymatically *via* scattering and transmitted light captured by a smartphone camera. RGB scattering intensities processed on Image J software and 20–100 μM range of linearity were reported between the green absorption (ΔI_{A-T}) light intensity and glucose concentration.[122] In the presence of GOx, the side product of the reaction is H_2O_2 that etches the AgNPrs causing color changes in the solution. In this case, no chromogenic agent was needed. The restrictive factors in studies with enzymes are the high cost of their fabrication and purification, certain working temperatures, short shelf life, *etc.*, that motivate the generation of new alternative systems with smartphone applications.[141] The temperature of 37 °C and pH 7.0 value are the maximal catalytic activities for enzymes,[142] and the result is affected by these parameters. Therefore, novel structures and materials are being investigated as an alternative to enzymes. Nanomaterials are the subject of intense current research interest for biomedical applications due to their tunable structures/activities, and ease of preparation. Nanomaterial based artificial enzymes (nanozymes) have the potential to act as

oxidase or peroxidase mimics.[143] Fe_3O_4,[144] AuNPs,[145] CeO_2,[146] MoS_2 nanoparticles,[147,148] CuO,[149] Co_3O_4 nanoparticles,[150] carbon-based nanomaterials,[151–155] layered double hydroxide,[156] and magnetic nanoparticles (MNPs)[157,158] can be used as artificial enzymes instead of natural enzymes, where advantages such as low cost, high stability, robustness, tunable catalytic activity, *etc*. are appealing.[141] Moreover, lower LOD values for glucose detection have been achieved by increasing the catalytic performance obtained due to the synergistic effects of the combined nanozyme structures.[159] It was proven that the synergistic effect increases both the binding interaction of glucose to the metal as well as the adsorbed oxygen in the analyte, resulting in enhanced electron transfer.[160] However, the uncertain mechanisms of the interactions, the complicated synthesis of materials, the costs and nanotoxicity of some structures, the composition, size, and shape dependent catalytic activity are factors that limit their use.[141]

Metal oxide frameworks (MOFs) have porous architectures potentially similar to natural enzymes.[161] It is possible to prepare MOFs that are able to catalyze oxidation reactions in the presence of H_2O_2 to imitate the peroxidase enzyme.[162–165] TMB is oxidized by H_2O_2 in the presence of a MOF on which the resulting reaction turns blue-green. The capturing conditions of the color changes were kept constant by placing the smartphone in a wooden box with two LED 6500 K lamps. Glucose determination was performed by regarding the S value of HSV changes, resulting in a limit of detection of 2.5 μmol L^{-1}.[121] As seen in Fig. 11A, another peroxidase mimic has been used on a designed filter paper system for glucose detection by highly stable antimony doped tin oxide (ATO) nanoparticles. The blue-green color (Fig. 11B) was captured with a smartphone by transferring to Image J software to analyze the images by the mean gray value, and the LOD value was found to be 21 μM (Fig. 11C).[115] A nanocomposite system based on Co_3O_4–CeO_2 was synthesized by the hydrothermal method and was used instead of peroxidase. The color changes on the paper-based analytical device (PAD) were subsequently monitored by the Color Picker software installed on a smartphone, and a LOD value of 0.21 μM was observed (Fig. 11D and E). Besides, the method offers a high selectivity for glucose against DNA, BSA, $CaCI_2$, NaCl, $MgCI_2$, ascorbic acid, and uric acid which can be seen in Fig. 11F.[71]

The purpose of synthesizing new ones among nanomaterials mimicking natural enzymes and testing them in glucose determination is to increase sensitivity which is possible with the highest affinity and catalytic activity towards TMB. For this purpose, glucose determination was achieved by an enzyme mimetic $MnFe_2O_4$/g-C_3N_4 (graphitic carbon nitride) nanocomposite material which oxidized colorless TMB to a blue-colored product in the presence of H_2O_2.[166] The LOD was

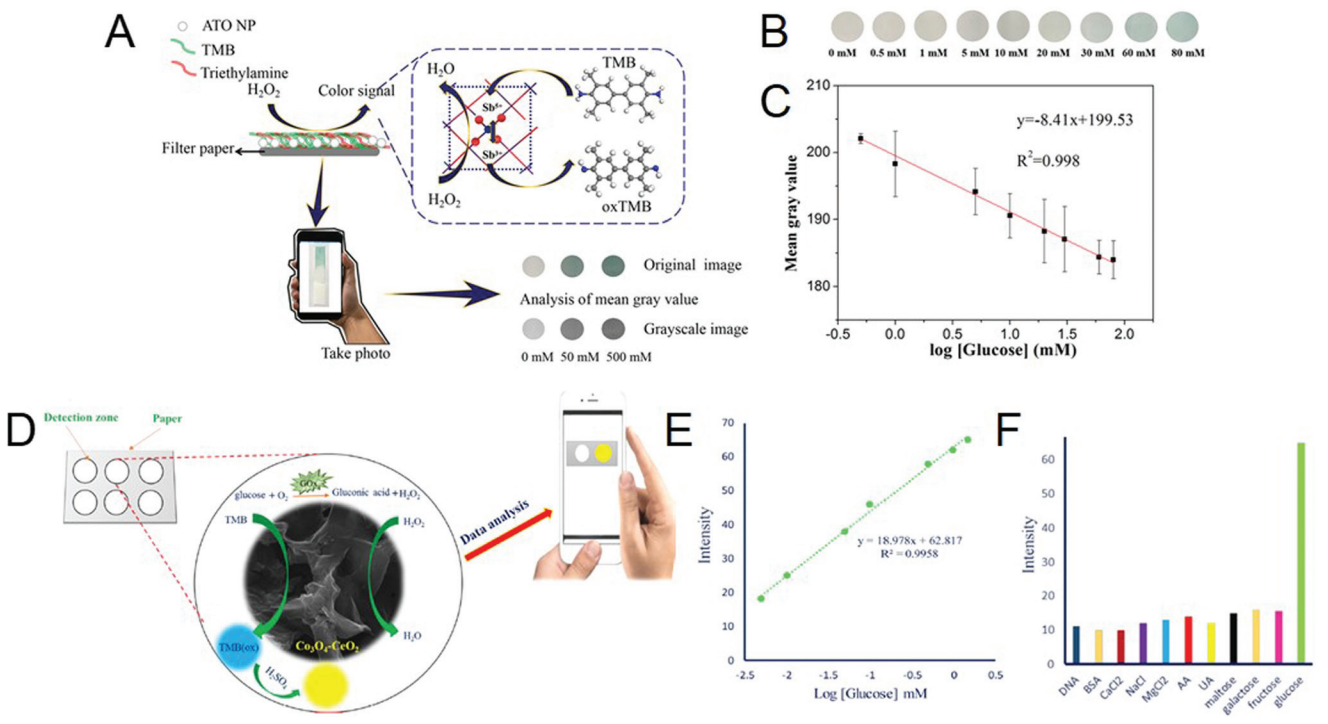

Fig. 11 (A) Schematic presentation of the ATO-based paper assay. (B) Image of the ATO-based filter paper after its reaction with different concentrations of glucose (after the glucose reacting with GOx). (C) Calibration plot of the paper-based sensor to different concentrations of glucose. Reproduced from ref. 115, Copyright 2019 with permission from Springer. (D) Schematic of the illustration and assay procedure of glucose detection on the paper-based chip. (E) The glucose calibration curve plotted on a logarithmic scale. (F) The selectivity of the proposed biosensor toward different interferences. Reproduced from ref. 71, Copyright 2019 with permission from Elsevier.

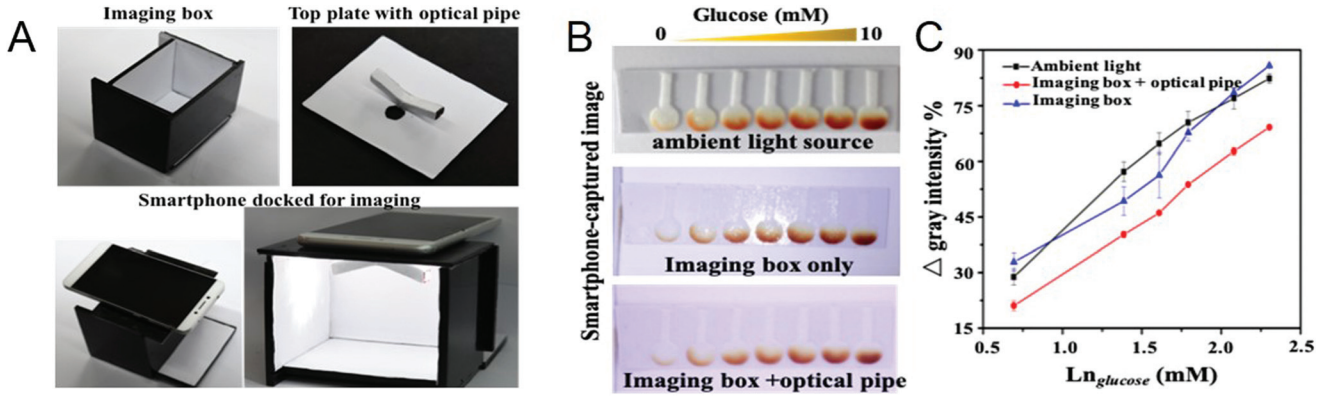

Fig. 12 (A) 3D printed and assembled imaging box. Analytical performance of smartphone-based colorimetric detection of glucose; (B) smartphone captured glucose testing on paper strips; (C) dose-signal curves of colorimetric based glucose detection. Reproduced from ref. 119, Copyright 2019 with permission from Elsevier.

determined as 17.3 nM using a UV-Vis spectrometer. An artificial neural network-based application was used and color changes were imaged by a smartphone camera. It is aimed to test the glucose concentration of the relationships between the RGB data by using an artificial neural network in the study, which generally causes lower accuracy as a result of using one of the red, green and blue channels and neglecting the others.

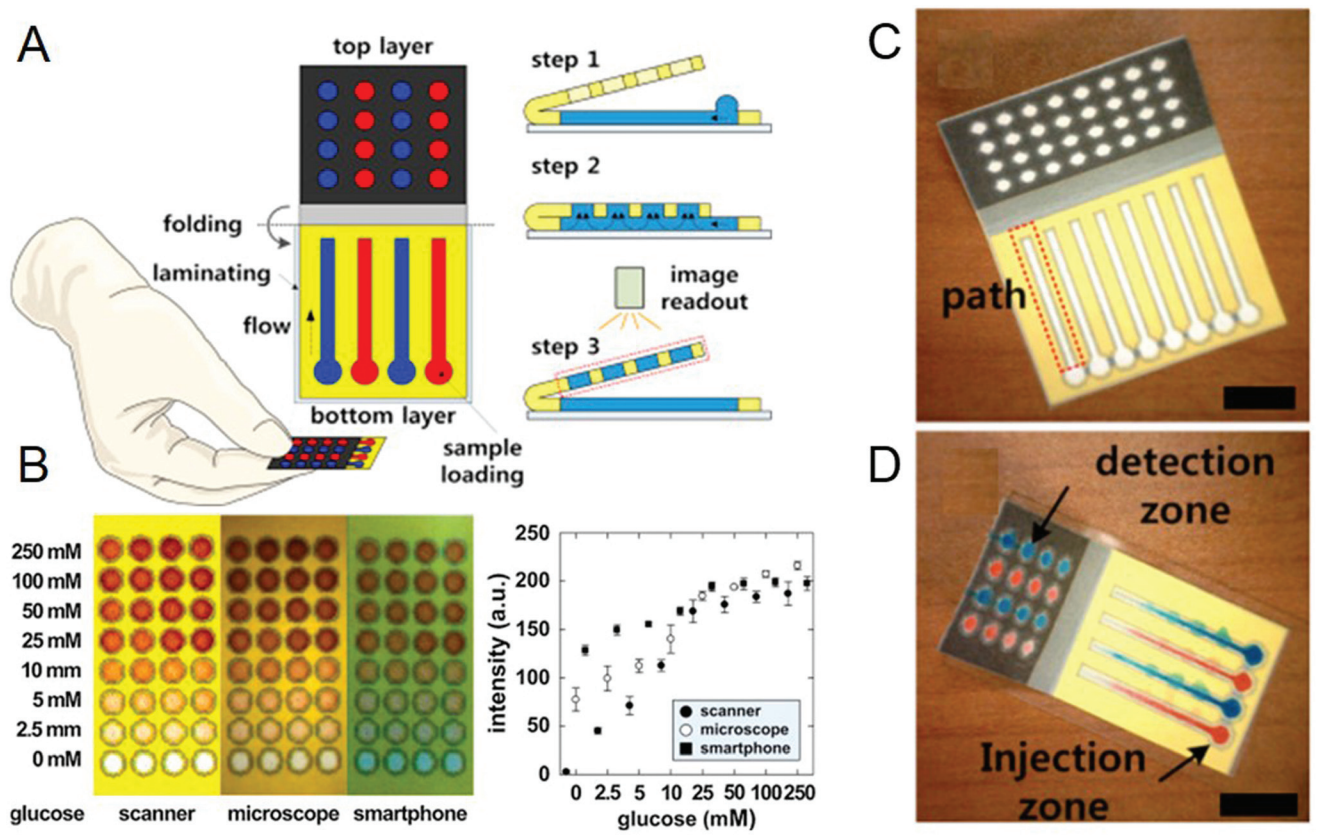

Fig. 13 (A) Paper-based 3D microfluidic device for multiple bioassays and sequential fluidic manipulation. The device consists of two layers. (B) Colorimetric bioassays and intensity analyses of glucose concentrations with three image readout instruments. Calibration curves for glucose concentrations of 0–50 mM were R^2 = 0.9781 for the scanner, 0.9686 for the microscope, and 0.9658 for the smartphone, respectively. (C) Paper-based 3D microfluidic devices with 32 reservoirs. (D) The origami-driven paper-based microfluidic platform operating principle was tested by injection of Methylene Blue and Congo Red in water. Reproduced from ref. 124, Copyright 2015 with permission from Elsevier.

7. Recent developments in highly sensitive glucose sensors

The technological developments have provided new alternatives to current glucose monitoring methods at an increasing rate. Considering the number of people who have access to smartphones and the services they provide, facilitating the determination of diabetes using these devices will provide great convenience. The methods using 3D-printed, screen-printed, and polymer templates allow performing multiple analyses to save time and cost. The simplicity of the method, response time, stability, robustness, selectivity, and sensitivity are the most critical parameters.

7.1. 3-D printed materials

The use of a 3-dimensional printer has gained attention due to its potential advantages in converting designs to prototypes for testing (and potentially manufacture if successful) at a low cost. The main purpose of these newly designed systems is to increase analytical performance by exploiting the imaging capacity for the enhancement of the accuracy of smartphone cameras. The imaging box was developed by adding a V-shaped tube fabricated using a 3-D printer to avoid ambient light interference directing a smartphone light as seen in Fig. 12A.[119] As proof of the contribution to analytical performance, 0.83 mM glucose determination limit under ambient conditions was reduced to 0.67 mM with the imaging box. Moreover, it was reduced to 0.13 mM with the use of a V-shaped optical tube preventing the reflection of light from the surface of the target.

The color change obtained by the enzymatic reaction was captured with a smartphone (Fig. 12B). The analysis of the gray-level intensities was carried out with Image J. Thus, the detection limit of the glucose detected by the system was improved by using imaging box and V-shaped tube produced by a 3-D printer (Fig. 12C). As the design of the device is critical to the architecture of the system, the practical use of the 3D printers stands out to enable rapid prototyping and subsequent manufacture.

7.2. Screen-printed electrodes

Screen-printed electrodes (SPEs) are preferred in biosensor applications because they are simple, inexpensive, reproducible, and disposable and can be mass-produced. They can be easily modified and thus allow the determination of different analytes.[167,168] It is also advantageous to combine screen-printing and wax-printing to obtain hydrophobic surfaces with non-toxic chemicals on substrates including plastic, ceramic, metal, and paper.[169,170] As seen in Fig. 13, wax-printed foldable, Slip-PAD designed, origami-driven paper-based 3D microfluidic chips are used for glucose detection by placing on the top layer the biological assays and on the bottom layer the

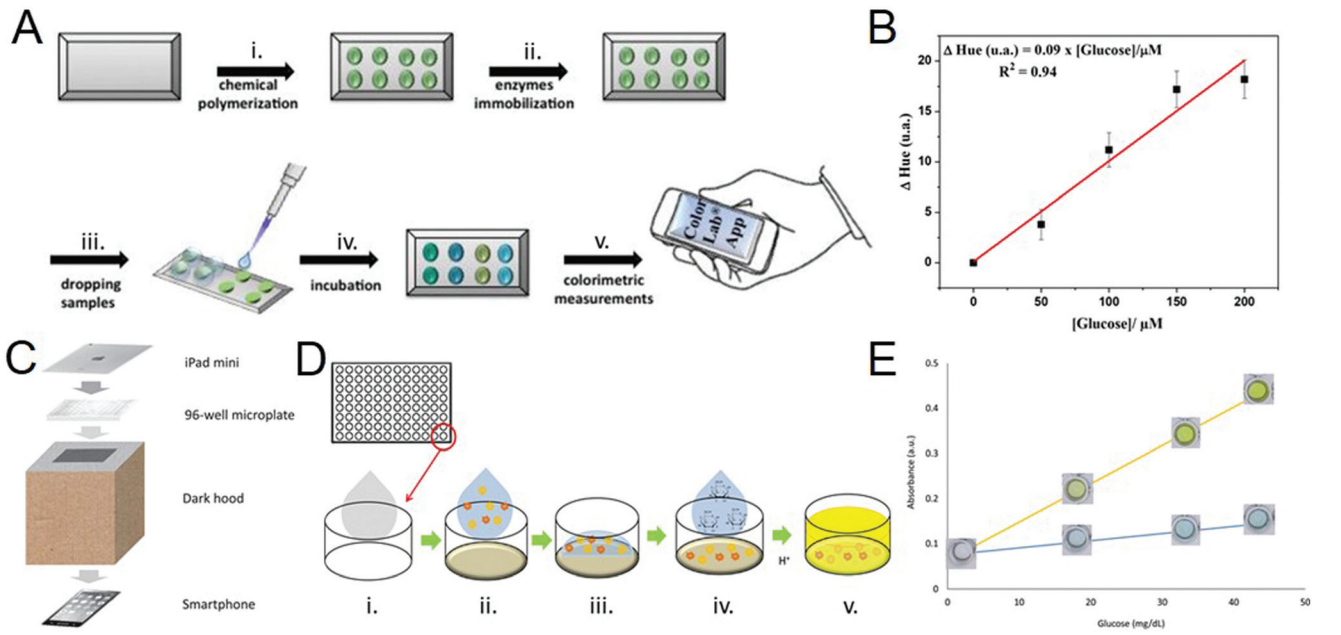

Fig. 14 (A) Scheme of the multiplexed enzymatic assay; (i) aniline and anthranilic acid chemically co-polymerized on the polyester substrate; (ii) enzymes immobilization by spotting the solutions onto the substrate; (iii) dropping samples; (iv) incubation with samples; (v) capture of the colorimetric change using the smartphone's camera (B) calibration plots analyzed by ColorLab®, a smartphone application. Reproduced from ref. 125, Copyright 2019 with permission from Elsevier. (C) Schematic representation of the system applied to carry out the measurements. (D) Illustration of the fabrication process and detection principle of the glucose sensor. (i) Introduction of the mixture composed of PDMS–TEOS–SiO_2 NPs-TMB in each well. (ii) Addition of the enzymes HRP and GOx. (iii) Evaporation of the water. (iv) Addition of the buffer and the glucose. (v) Change of color produced by the oxidation of the TMB. (E) Comparison between the calibrates obtained before and after acidifying the solutions. Reproduced from ref. 126, Copyright 2018 with permission from Elsevier.

samples. The foldable design gives the advantage of detecting the color changes using three different instruments, with good results obtained for the scanner (Epson), microscope, and smartphone, respectively. This system can be detected at the glucose level, which is in the clinical range between 0 and 900 mg dL^{-1}. However, a calibration that compensates the error that may occur in photographs taken under ambient light conditions has not been applied for the smartphone or microscope.[124]

7.3. Polymer templates

Polymer matrices are used to perform enzymatic reactions on a solid substrate which opens the way to produce disposable glucose meters. Transparent porous structures are a good template for biomolecules which can be formed by polydimethylsiloxane with pore size distribution controlled with cross-linkers (triethoxymethylsilane (MTEOS) or tetraethylorthosilicate (TEOS)).[171] A poly(aniline-*co*-anthranilic acid) (ANI-*co*-AA) composite film has been used for enzyme immobilization with HRP, GOx, GOx-HRP, and tyrosinase (Tyr). Due to the good electrical and optical properties of aniline, the matrix was formed for enzyme immobilization by copolymerization of aniline with *o*-anthranilic acid to increase the solubility in the solvents.[172] The color imaging analysis has been performed on Android-based ColorLab® application with a 20 μM LOD for glucose, as seen in Fig. 14A and B.[125] A polymeric support system (PDMS–TEOS–SiO_2NPs) plays a role in immobilizing the system shown in Fig. 14 with all reagents in a 96-well microplate achieved by smartphone-based technology. The limit of detection was 1.8 mg dL^{-1}, and the system has good linearity in the range of 6–88 mg dL^{-1}. The system was constructed up in a dark hood and iPad Mini display used as a backlight by My Light application for the microplates. The images were taken with a smartphone, processed in Image J, and it was found that the yellow color blue channel intensity was more suitable in the RGB color mode. For this reason, to increase the sensitivity, the solution was acidified to obtain a yellow color.[126]

Glucose determination was performed in a 200 μL volume channel prepared using PDMS upper and PET bottom layers. An optical signal transducer colorimetric biosensor was developed in which the determined glucose concentration was in the range between 0 and 10 mM. Built on signal transmission technology consisting of a smartphone and a computer monitor, the conversion of light intensity to signals can be detected by the naked eye. In this optical signal converter system, the computer screen acts as a light source and a signal guide generator, while a smartphone is used as an optical

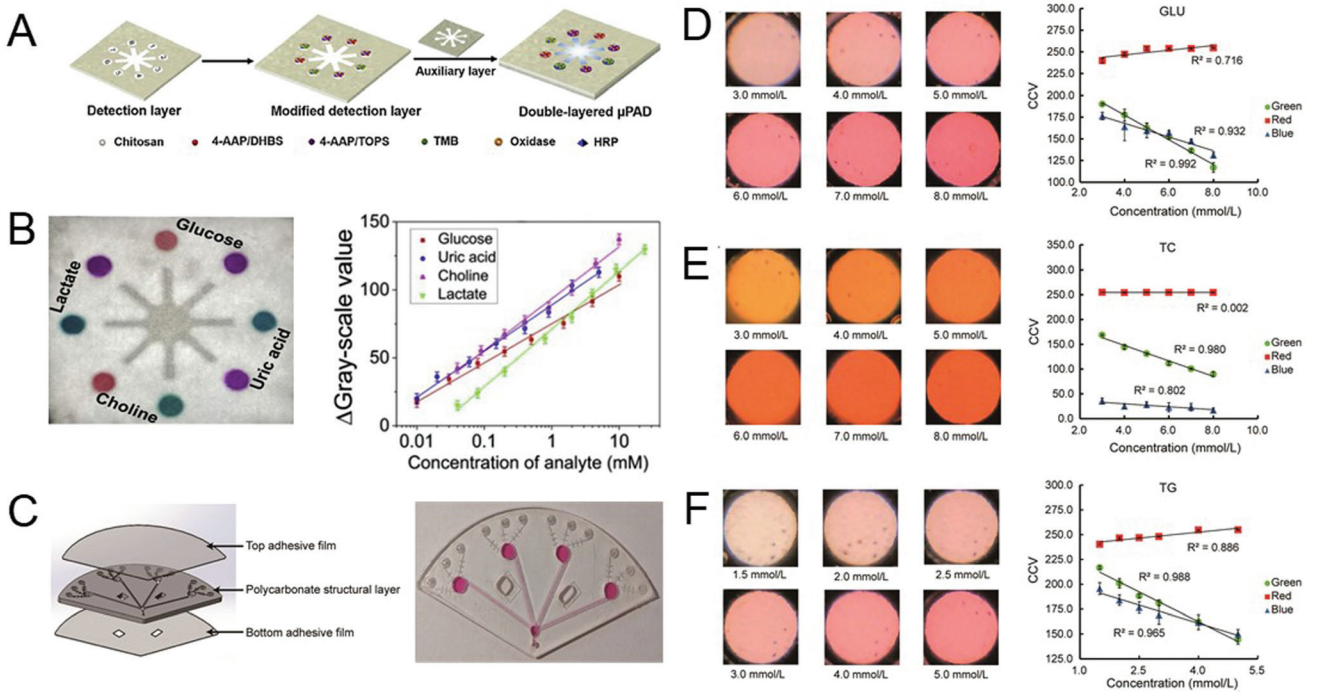

Fig. 15 (A) Schematic illustration of the fabrication of the double-layered μPADs with multiple indicators for the simultaneous detection of four analytes. (B) Left: Color photograph of the detection layer of the double-layered 3D μPAD. Right: Representative calibration curves for the detection of glucose, uric acid, choline and lactate by using the double-layered μPAD. Reproduced from ref. 129, Copyright 2019 with permission from Elsevier. (C) Enlarged view of the microchip. (D) Left: Captured images of a series of glucose solutions in the concentration range of 3.0–8.0 mmol L^{-1} detected in the microchip. Right; the linear fittings between the concentrations of GLU and the color characteristic value of the Red/Green/Blue channels of the images. (E) Left: Images of the total cholesterol solutions (3.0–8.0 mmol L^{-1}) analyzed in the chip. Right; the corresponding linear fittings. (F) Left: Images with the linear fittings of the triglyceride solutions (1.5–5.0 mmol L^{-1}). Right: The corresponding linear fittings. Reproduced from ref. 130, Copyright 2019 with permission from Elsevier.

receiver and signal display. The increasing number of edges of each polygon was correlated with analyte concentration.[127] The methods that allow the detection of small amounts of samples are popular, especially with the development of extracting technologies from the body fluids. In one of these methods, the embossed-paper microfluidic device was developed and the analyte flow was facilitated from the waterproof hydrophilic paper *via* a hollow channel. In order to provide these two properties together, the paper is designed to have two-layers. The first layer is styrene–butadiene rubber (SBR), and the second is poly(vinyl alcohol) (PVA) or copolymer styrene-acrylic (SA). Spontaneous capillary flow occurred through the layers. While the color change can be observed by the naked eye, the images taken by the smartphone are also processed in Image J.[128]

7.4. Designs for multiple analyses

Multiple analysis systems have been created to save time and cost for analyzing multiple samples at the same time or for the analysis of different samples of the same analyte. A double layer μPAD shown in Fig. 15A was designed to develop a multi-colorimeter system for the determination of uric acid, lactate and choline as well as glucose (Fig. 15B). The enzymatic glucose determination was performed with iPhone 6, and images were transferred to Image J for processing. Hue values were determined by Photoshop software, and the gray-scale value was found to be ideal for four analytes. In this calibration curve, the graph has been drawn for glucose detection between the range of 0.01 and 10.0 mmol L^{-1}.[129] As seen in Fig. 15C–F, a multi-index system of fan-shaped microfluidics as another monitoring method was developed to perform glucose, triglyceride and cholesterol analysis. Enzymatic glucose determination was performed by processing RGB values using an LED light source and CCD camera. Green and blue linearity are higher than others, and reproducible results are obtained for each analyte in the green channel.[130]

8. Conclusion and future outlook

In this review, smartphone-based colorimetric glucose detection was examined based on different methods and analytes. These methods have been evolved from invasive to non-invasive and use body fluids such as sweat, tears, urine, saliva, and interstitial fluid. With the advances in smartphone technology, the accuracy of glucose detection has been improved significantly. Through electronic and optical biosensors integrated into wearable devices, *e.g.* patches, tattoos, stamps, wristbands, or contact lenses, the body fluids can be analyzed after the physical and biochemical data are received from the sensors. Moreover, bioanalytes and nanostructures can be used either enzymatically or non-enzymatically in glucose detection. Due to stability issues during transport and storage in enzymatic glucose measurement, non-enzymatic methods have gained prevalence in the last decade. However, smartphone-based studies using non-enzymatic methods are still at a nascent stage. In addition, advanced methods using 3-D printed materials, screen-printed electrodes, polymer templates, and practical designs for multiple analyses have been developed to enhance the sensitivity of smartphone-based sensors for glucose measurement. The new hardware systems in smartphone-based platforms are emerging as personal health management tools that can be operated in resource-limited and developing world settings, while sophisticated software methods like artificial intelligence (AI) are trending due to their potential applications in data processing. Machine learning and deep learning, which are subsets of AI, will be the dominant method for a long time due to their powerful utilities such as automated decision-making and self-learning from the data. The advantageous combination of sophisticated software methods and new hardware systems will revolutionize the concept of the smartphone-based platform from glucose measurement to personal health management. Ultimately, the advances in translation of hardware and software technologies into practical, field-deployable, cost-effective, user-friendly, portable, and commercially available products will ensure the success of future smartphone-based platforms.

Conflicts of interest

There are no conflicts to declare.

Acknowledgements

This research was supported by the Scientific and Technological Research Council of Turkey (TUBITAK)–British Council (The Newton-Katip Celebi Fund Institutional Links, Turkey-UK project: 116E934) and the Scientific Research Projects Coordination unit of Izmir Katip Celebi University (Project No. 2018-ÖDL-MÜMF-0021).

References

1 W. H. Organization, *Diabetes*, 2020, https://www.who.int/health-topics/diabetestab=tab1.
2 S. L. Cowart and M. E. Stachura, *Clinical Methods: The History, Physical, and Laboratory Examinations. 3rd edition*, Butterworths, 1990.
3 L. C. Clark Jr. and C. Lyons, *Ann. N. Y. Acad. Sci.*, 1962, **102**, 29–45.
4 B. Schersten, C. Kuhl, A. Hollender and R. Ekman, *Br. Med. J.*, 1974, **3**, 384–387.
5 A. Albisser, B. Leibel, T. Ewart, Z. Davidovac, C. Botz and W. Zingg, *Diabetes*, 1974, **23**, 389–396.
6 M. Shichiri, Y. Yamasaki, R. Kawamori, N. Hakui and H. Abe, *Lancet*, 1982, **320**, 1129–1131.
7 A. Clemens, P. Chang and R. Myers, *Horm. Metab. Res.*, 1977, 23–33.
8 D. Matthews, R. Holman, E. Bown, J. Steemson and A. Watson, *Lancet*, 1987, **1**, 778–779.

9 J. J. Mastrototaro, *Diabetes Technol. Ther.*, 2000, **2**, 13–18.
10 M. Tierney, J. Tamada, R. Potts, L. Jovanovic, S. Garg and Cygnus Research Team, *Biosens. Bioelectron.*, 2001, **16**, 621–629.
11 V. Franklin, A. Waller, C. Pagliari and S. Greene, *Diabetes Technol. Ther.*, 2003, **5**, 991–996.
12 A. Farmer, O. Gibson, P. Hayton, K. Bryden, C. Dudley, A. Neil and L. Tarassenko, *J. Innov. Health Inform.*, 2005, **13**, 171–177.
13 C. Rabin and B. Bock, *Telemed. e-Health*, 2011, **17**, 801–803.
14 A. A. Nes, S. Van Dulmen, E. Eide, A. Finset, Ó. B. Kristjánsdóttir, I. S. Steen and H. Eide, *Diabetes Res. Clin. Pract.*, 2012, **97**, 385–393.
15 T. Gölcez, V. Kiliç and M. Şen, 2019 Medical Technologies Congress (TIPTEKNO), 2019, pp. 1–4.
16 T. Golcez, V. Kilic and M. Sen, *Anal. Sci.*, 2020, 20P262.
17 Ö. B. Mercan, V. Kılıç and M. Şen, *Sens. Actuators, B*, 2020, 129037.
18 GlucoWise, MediWise Ltd., UK, January 2021, https://gluco-wise.com/.
19 DiaMonTech, January 2021, https://www.diamontech.de/home.
20 OrSense, January 2021, https://www.medgadget.com/2006/12/noninvasiveglu.html.
21 G. Cappon, M. Vettoretti, G. Sparacino and A. Facchinetti, *Diabetes Metab. J.*, 2019, **43**, 383–397.
22 Y. Uwadaira and A. Ikehata, *Nutritional and Therapeutic Interventions for Diabetes and Metabolic Syndrome*, Elsevier, 2018, pp. 489–504.
23 G. K. Özdemir, A. Bayram, V. Kilic, N. Horzum and M. E. Solmaz, *Anal. Methods*, 2017, **9**, 579–585.
24 A. Y. Mutlu, V. Kilic, G. K. Özdemir, A. Bayram, N. Horzum and M. E. Solmaz, *Analyst*, 2017, **142**, 2434–2441.
25 D. Akkaynak, T. Treibitz, B. Xiao, U. A. Gürkan, J. J. Allen, U. Demirci and R. T. Hanlon, *J. Opt. Soc. Am. A*, 2014, **31**, 312–321.
26 A. K. Yetisen, J. Martinez-Hurtado, A. Garcia-Melendrez, F. da Cruz Vasconcellos and C. R. Lowe, *Sens. Actuators, B*, 2014, **196**, 156–160.
27 M.-Y. Jia, Q.-S. Wu, H. Li, Y. Zhang, Y.-F. Guan and L. Feng, *Biosens. Bioelectron.*, 2015, **74**, 1029–1037.
28 Y. Zhang, Y. Wu, Y. Zhang and A. Ozcan, *Sci. Rep.*, 2016, **6**, 27811.
29 Ö. B. Mercan, *et al.*, *2020 Medical Technologies Congress (TIPTEKNO)*, 2020, pp. 1–4.
30 C. Sun, J. C. Malcolm, B. Wong, R. Shorr and M.-A. Doyle, *Can. J. Diabetes*, 2019, **43**, 51–58.
31 R. Shan, S. Sarkar and S. S. Martin, *Diabetologia*, 2019, **62**, 877–887.
32 O. Kordonouri and M. C. Riddell, *Ther. Adv. Endocrinol. Metab.*, 2019, **10**, 2042018819839298.
33 M. M. Kebede, C. Schuett and C. R. Pischke, *J. Clin. Med.*, 2019, **8**, 109.
34 J. Doupis, G. Festas, C. Tsilivigos, V. Efthymiou and A. Kokkinos, *Diabetes Ther.*, 2020, 1–13.
35 J. Pavlas, O. Krejcar, P. Maresova and A. Selamat, *Computers*, 2019, **8**, 1.
36 H.-C. Wang, F.-Y. Chang, T.-M. Tsai, C.-H. Chen and Y.-Y. Chen, *Biomed. Opt. Express*, 2020, **11**, 2166–2177.
37 A. Bayram, N. Horzum, A. U. Metin, V. Kılıç and M. E. Solmaz, *IEEE Sens. J.*, 2018, **18**, 5948–5955.
38 V. Kilic, G. Alankus, N. Horzum, A. Y. Mutlu, A. Bayram and M. E. Solmaz, *ACS Omega*, 2018, **3**, 5531–5536.
39 M. E. Solmaz, A. Y. Mutlu, G. Alankus, V. Kilic, A. Bayram and N. Horzum, *Sens. Actuators, B*, 2018, **255**, 1967–1973.
40 V. Kiliç and M. Şen, 2019 Medical Technologies Congress (TIPTEKNO), 2019, pp. 1–4.
41 Ö. B. Mercan and V. Kılıç, International Conference on Intelligent and Fuzzy Systems, 2020, pp. 1276–1283.
42 S. Singhal, P. Ralhan and N. Jatana, 2015 Eighth International Conference on Contemporary Computing (IC3), 2015, pp. 269–274.
43 T.-T. Wang, C. kit Lio, H. Huang, R.-Y. Wang, H. Zhou, P. Luo and L.-S. Qing, *Talanta*, 2020, **206**, 120211.
44 K. Sun, Y. Yang, H. Zhou, S. Yin, W. Qin, J. Yu, D. T. Chiu, Z. Yuan, X. Zhang and C. Wu, *ACS Nano*, 2018, **12**, 5176–5184.
45 M. M. Baig, H. GholamHosseini and M. J. Connolly, *Australas. Phys. Eng. Sci. Med.*, 2015, **38**, 23–38.
46 K. Pahlavan and P. Krishnamurthy, *Principles of Wireless Networks: A Unified Approach*, Prentice Hall PTR, 2011.
47 U. Mitra, B. A. Emken, S. Lee, M. Li, V. Rozgic, G. Thatte, H. Vathsangam, D.-S. Zois, M. Annavaram, S. Narayanan, *et al.*, *IEEE Commun. Mag.*, 2012, **50**, 116–125.
48 S. Ullah, H. Higgins, B. Braem, B. Latre, C. Blondia, I. Moerman, S. Saleem, Z. Rahman and K. S. Kwak, *J. Med. Syst.*, 2012, **36**, 1065–1094.
49 Y. Lan, Y. Kuang, L. Zhou, G. Wu, P. Gu, H. Wei and K. Chen, *Laser Phys. Lett.*, 2017, **14**, 035603.
50 Q. Lu, T. Huang, J. Zhou, Y. Zeng, C. Wu, M. Liu, H. Li, Y. Zhang and S. Yao, *Spectrochim. Acta, Part A*, 2021, **244**, 118893.
51 Z. Liu, L. Liu, M. Sun and X. Su, *Biosens. Bioelectron.*, 2015, **65**, 145–151.
52 S. Hu, Y. Jiang, Y. Wu, X. Guo, Y. Ying, Y. Wen and H. Yang, *ACS Appl. Mater. Interfaces*, 2020, **12**, 55324–55330.
53 Q.-H. Phan, T.-H. Jian, Y.-R. Huang, Y.-R. Lai, W.-Z. Xiao and S.-W. Chen, *Opt. Lasers Eng.*, 2020, **134**, 106268.
54 S. Emaminejad, W. Gao, E. Wu, Z. A. Davies, H. Y. Y. Nyein, S. Challa, S. P. Ryan, H. M. Fahad, K. Chen, Z. Shahpar, *et al.*, *Proc. Natl. Acad. Sci. U. S. A.*, 2017, **114**, 4625–4630.
55 J. Y. Sim, C.-G. Ahn, E.-J. Jeong and B. K. Kim, *Sci. Rep.*, 2018, **8**, 1–11.
56 H. Chen, X. Chen, S. Ma, X. Wu, W. Yang, W. Zhang and X. Li, *J. Infrared, Millimeter, Terahertz Waves*, 2018, **39**, 399–408.
57 A. E. Omer, G. Shaker, S. Safavi-Naeini, H. Kokabi, G. Alquié, F. Deshours and R. M. Shubair, *Sci. Rep.*, 2020, **10**, 1–20.

58 S. T. Doherty and P. Oh, *Telemed. e-Health*, 2012, **18**, 185–192.
59 A. Rghioui, J. Lloret, M. Harane and A. Oumnad, *Electronics*, 2020, **9**, 678.
60 D.-A. Antonovici, I. Chiuchisan, O. Geman and A. Tomegea, 2014 International Symposium on Fundamentals of Electrical Engineering (ISFEE), 2014, pp. 1–4.
61 A. Menon, F. Fatehi, D. Bird, D. Darssan, M. Karunanithi, A. Russell and L. Gray, *Int. J. Environ. Res. Public Health*, 2019, **16**, 959.
62 L. I. Corp, *Thriving with Diabetes*, 2020, http://mydario.com/.
63 Philosys, *Gmate Blood Glucose Monitoring System*, 2020, http://philosys.com/en/.
64 A. G. Aggidis, J. D. Newman and G. A. Aggidis, *Biosens. Bioelectron.*, 2015, **74**, 243–262.
65 W. Villena Gonzales, A. T. Mobashsher and A. Abbosh, *Sensors*, 2019, **19**, 800.
66 J. He, G. Xiao, X. Chen, Y. Qiao, D. Xu and Z. Lu, *RSC Adv.*, 2019, **9**, 23957–23963.
67 M. Wróbel, IOP Conference Series: Materials Science and Engineering, 2016, pp. l–9.
68 N. Li, H. Zang, H. Sun, X. Jiao, K. Wang, T. C.-Y. Liu and Y. Meng, *Molecules*, 2019, **24**, 1500.
69 A. Sieg, R. H. Guy and M. B. Delgado-Charro, *Diabetes Technol. Ther.*, 2005, **7**, 174–197.
70 M. Bariya, H. Y. Y. Nyein and A. Javey, *Nat. Electron.*, 2018, **1**, 160–171.
71 N. Alizadeh, A. Salimi and R. Hallaj, *Sens. Actuators, B*, 2019, **288**, 44–52.
72 M. C. Brothers, M. DeBrosse, C. C. Grigsby, R. R. Naik, S. M. Hussain, J. Heikenfeld and S. S. Kim, *Acc. Chem. Res.*, 2019, **52**, 297–306.
73 J. Moyer, D. Wilson, I. Finkelshtein, B. Wong and R. Potts, *Diabetes Technol. Ther.*, 2012, **14**, 398–402.
74 H. Lee, C. Song, Y. S. Hong, M. S. Kim, H. R. Cho, T. Kang, K. Shin, S. H. Choi, T. Hyeon and D.-H. Kim, *Sci. Adv.*, 2017, **3**, e1601314.
75 Z. Zhang, M. Azizi, M. Lee, P. Davidowsky, P. Lawrence and A. Abbaspourrad, *Lab Chip*, 2019, **19**, 3448–3460.
76 A. K. Yetisen, R. Moreddu, S. Seifi, N. Jiang, K. Vega, X. Dong, J. Dong, H. Butt, M. Jakobi, M. Elsner, *et al.*, *Angew. Chem.*, 2019, **131**, 10616–10623.
77 T. Rönnemaa and V. A. Koivisto, *Diabetes Care*, 1988, **11**, 769–773.
78 G. Xiao, J. He, X. Chen, Y. Qiao, F. Wang, Q. Xia, L. Yu and Z. Lu, *Cellulose*, 2019, **26**, 4553–4562.
79 R. Moreddu, J. S. Wolffsohn, D. Vigolo and A. K. Yetisen, *Sens. Actuators, B*, 2020, 128183.
80 L. Yu, Z. Yang and M. An, *BioSci. Trends*, 2019, **13**, 308–313.
81 K. M. Daum and R. M. Hill, *Invest. Ophthalmol. Visual Sci.*, 1982, **22**, 509–514.
82 J. T. Baca, D. N. Finegold and S. A. Asher, *Ocul. Surf.*, 2007, **5**, 280–293.
83 D. Sen and G. Sarin, *Br. J. Ophthalmol.*, 1980, **64**, 693–695.
84 X. Wang, F. Li, Z. Cai, K. Liu, J. Li, B. Zhang and J. He, *Anal. Bioanal. Chem.*, 2018, **410**, 2647–2655.
85 D. Bruen, C. Delaney, L. Florea and D. Diamond, *Sensors*, 2017, **17**, 1866.
86 U. M. Jalal, G. J. Jin and J. S. Shim, *Anal. Chem.*, 2017, **89**, 13160–13166.
87 T.-T. Wang, K. Guo, X.-M. Hu, J. Liang, X.-D. Li, Z.-F. Zhang, J. Xie, *et al.*, *Chemosensors*, 2020, **8**, 10.
88 A. S. Panchbhai, *J. Oral. Maxillofac. Surg.*, 2012, **3**, 1–7.
89 V. E. Coyle, A. E. Kandjani, M. R. Field, P. Hartley, M. Chen, Y. M. Sabri and S. K. Bhargava, *Biosens. Bioelectron.*, 2019, 111479.
90 L. F. de Castro, S. V. de Freitas, L. C. Duarte, J. A. C. de Souza, T. R. Paixão and W. K. Coltro, *Anal. Bioanal. Chem.*, 2019, 1–10.
91 P. Chakraborty, S. Dhar, N. Deka, K. Debnath and S. P. Mondal, *Sens. Actuators, B*, 2020, **302**, 127134.
92 N. Fakhri, F. Salehnia, S. M. Beigi, S. Aghabalazadeh, M. Hosseini and M. R. Ganjali, *Microchim. Acta*, 2019, **186**, 385.
93 S. Gupta, M. T. Nayak, J. Sunitha, G. Dawar, N. Sinha and N. S. Rallan, *J. Oral Maxillofac. Pathol.*, 2017, **21**, 334.
94 Y. Jia, H. Sun, X. Li, D. Sun, T. Hu, N. Xiang and Z. Ni, *Biomed. Microdevices*, 2018, **20**, 89.
95 A. Soni and S. K. Jha, *Anal. Chim. Acta*, 2017, **996**, 54–63.
96 A. Soni and S. K. Jha, *Biosens. Bioelectron.*, 2015, **67**, 763–768.
97 N. Fogh-Andersen, B. M. Altura, B. T. Altura and O. Siggaard-Andersen, *Clin. Chem.*, 1995, **41**, 1522–1525.
98 J. Hall, *J. Chem. Inf. Model.*, 2011, 973–986.
99 A. Basu, S. Dube, M. Slama, I. Errazuriz, J. C. Amezcua, Y. C. Kudva, T. Peyser, R. E. Carter, C. Cobelli and R. Basu, *Diabetes*, 2013, **62**, 4083–4087.
100 Y. Liu, B. Huang and Y. Yao, 2012 IEEE International Conference on Mechatronics and Automation, 2012, pp. 647–652.
101 J. Kim, J. R. Sempionatto, S. Imani, M. C. Hartel, A. Barfidokht, G. Tang, A. S. Campbell, P. P. Mercier and J. Wang, *Adv. Sci.*, 2018, **5**, 1800880.
102 H. Park, J.-Y. Lee, D.-C. Kim, Y. Koh and J. Cha, International Conference on Nano-Bio Sensing, Imaging, and Spectroscopy 2017, 2017, p. 1032405.
103 D. Li, B. Lu, R. Zhu, H. Yu and K. Xu, *Biomicrofluidics*, 2016, **10**, 011913.
104 P. P. Samant and M. R. Prausnitz, *Proc. Natl. Acad. Sci. U. S. A.*, 2018, **115**, 4583–4588.
105 H.-C. Wang, F.-Y. Chang, T.-M. Tsai, C.-H. Chen and Y.-Y. Chen, *J. Biomed. Opt.*, 2019, **24**, 027002.
106 M. M. Erenas, B. Carrillo-Aguilera, K. Cantrell, S. Gonzalez-Chocano, I. M. P. de Vargas-Sansalvador, I. de Orbe-Payá and L. F. Capitan-Vallvey, *Biosens. Bioelectron.*, 2019, **136**, 47–52.
107 Health Quality Ontario, *Ont. Health Technol. Assess. Ser.*, 2018, **18**(2), 1–160.

108 M. Muzny, A. Henriksen, A. Giordanengo, J. Muzik, A. Grøttland, H. Blixgård, G. Hartvigsen and E. Årsand, *Int. J. Med. Inf.*, 2019, 104017.
109 S. Seneviratne, Y. Hu, T. Nguyen, G. Lan, S. Khalifa, K. Thilakarathna, M. Hassan and A. Seneviratne, *IEEE Commun. Surv. Tutor.*, 2017, **19**, 2573–2620.
110 A. Hatamie, S. Angizi, S. Kumar, C. M. Pandey, A. Simchi, M. Willander and B. D. Malhotra, *J. Electrochem. Soc.*, 2020, **167**, 037546.
111 E. Ismar, S. Kurşun Bahadir, F. Kalaoglu and V. Koncar, *Glob. Challenges*, 2020, 1900092.
112 P. T. Toi, T. Q. Trung, T. M. L. Dang, C. W. Bae and N.-E. Lee, *ACS Appl. Mater. Interfaces*, 2019, **11**, 10707–10717.
113 H. Lee, Y. J. Hong, S. Baik, T. Hyeon and D.-H. Kim, *Adv. Healthcare Mater.*, 2018, **7**, 1–14.
114 B. J. Van Enter and E. Von Hauff, *Chem. Commun.*, 2018, **54**, 5032–5045.
115 Y. Li, J. Sun, W. Mao, S. Tang, K. Liu, T. Qi, H. Deng, W. Shen, L. Chen and L. Peng, *Microchim. Acta*, 2019, **186**, 403.
116 J. Zhou and T. Dong, *Analyst*, 2018, **143**, 2812–2818.
117 X. He, Q. Pei, T. Xu and X. Zhang, *Sens. Actuators, B*, 2020, **304**, 127415.
118 S. Shrestha, C. Harold, M. Boubin and L. Lawrence, *Smart Biomedical and Physiological Sensor Technology XV*, 2019, p. 110200R.
119 G. Chen, C. Fang, H. H. Chai, Y. Zhou, W. Y. Li and L. Yu, *Sens. Actuators, B*, 2019, **281**, 253–261.
120 O. Kublin and M. Stepień, *Clin. Diabetol.*, 2019, **8**, 121–126.
121 I. Ortiz-Gómez, A. Salinas-Castillo, A. G. García, J. A. Álvarez-Bermejo, I. de Orbe-Payá, A. Rodríguez-Diéguez and L. F. Capitán-Vallvey, *Microchim. Acta*, 2018, **185**, 47.
122 C. Lertvachirapaiboon, T. Maruyama, A. Baba, S. Ekgasit, K. Shinbo and K. Kato, *Anal. Sci.*, 2018, 18P412.
123 L. Chen, C. Zhang and D. Xing, *Sens. Actuators, B*, 2016, **237**, 308–317.
124 S. Choi, S.-K. Kim, G.-J. Lee and H.-K. Park, *Sens. Actuators, B*, 2015, **219**, 245–250.
125 O. Hosu, M. Lettieri, N. Papara, A. Ravalli, R. Sandulescu, C. Cristea and G. Marrazza, *Talanta*, 2019, **204**, 525–532.
126 J. Pla-Tolós, Y. Moliner-Martínez, C. Molins-Legua and P. Campíns-Falcó, *Sens. Actuators, B*, 2018, **258**, 331–341.
127 H. Chun, Y. Han, Y. Park, K. Kim, S. Lee and H. Yoon, *Materials*, 2018, **11**, 388.
128 D. Gosselin, M. Belgacem, B. Joyard-Pitiot, J. Baumlin, F. Navarro, D. Chaussy and J. Berthier, *Sens. Actuators, B*, 2017, **248**, 395–401.
129 F. Li, X. Wang, J. Liu, Y. Hu and J. He, *Sens. Actuators, B*, 2019, **288**, 266–273.
130 J. Li, Y. Sun, C. Chen, T. Sheng, P. Liu and G. Zhang, *Anal. Chim. Acta*, 2019, **1052**, 105–112.
131 D. Baş, *Anal. Methods*, 2017, **9**, 6698–6704.
132 Y. Wang, X. Liu, P. Chen, N. T. Tran, J. Zhang, W. S. Chia, S. Boujday and B. Liedberg, *Analyst*, 2016, **141**, 3233–3238.
133 Y. Wu, A. Boonloed, N. Sleszynski, M. Koesdjojo, C. Armstrong, S. Bracha and V. T. Remcho, *Clin. Chim. Acta*, 2015, **448**, 133–138.
134 H. J. Chun, Y. M. Park, Y. D. Han, Y. H. Jang and H. C. Yoon, *BioChip J.*, 2014, **8**, 218–226.
135 X. Wu, T. Chen, Y. Chen and G. Yang, *J. Mater. Chem. B*, 2020, **8**, 2650–2659.
136 X. Kou, L. Tong, Y. Shen, W. Zhu, L. Yin, S. Huang, F. Zhu, G. Chen and G. Ouyang, *Biosens. Bioelectron.*, 2020, **156**, 112095.
137 V. Kilic, N. Horzum and M. E. Solmaz, *Color Detection*, IntechOpen, 2018, pp. 1–19.
138 S. Liu and Y. Sun, *Biosens. Bioelectron.*, 2007, **22**, 905–911.
139 S. Ferri, K. Kojima and K. Sode, *Review of Glucose Oxidases and Glucose Dehydrogenases: A Bird's Eye View of Glucose Sensing Enzymes*, 2011.
140 Z. Tao, R. A. Raffel, A.-K. Souid and J. Goodisman, *Biophys. J.*, 2009, **96**, 2977–2988.
141 M. Liang and X. Yan, *Acc. Chem. Res.*, 2019, **52**, 2190–2200.
142 H. Bisswanger, *Perspect. Sci.*, 2014, **1**, 41–55.
143 H. Wei and E. Wang, *Chem. Soc. Rev.*, 2013, **42**, 6060–6093.
144 L. Gao, J. Zhuang, L. Nie, J. Zhang, Y. Zhang, N. Gu, T. Wang, J. Feng, D. Yang, S. Perrett, *et al.*, *Nat. Nanotechnol.*, 2007, **2**, 577.
145 Y. Hu, H. Cheng, X. Zhao, J. Wu, F. Muhammad, S. Lin, J. He, L. Zhou, C. Zhang, Y. Deng, *et al.*, *ACS Nano*, 2017, **11**, 5558–5566.
146 L. Jiang, Q. Xue, C. Jiao, H. Liu, Y. Zhou, H. Ma and Q. Yang, *Anal. Methods*, 2018, **10**, 2151–2159.
147 J. Yu, X. Ma, W. Yin and Z. Gu, *RSC Adv.*, 2016, **6**, 81174–81183.
148 K. Zhao, W. Gu, S. Zheng, C. Zhang and Y. Xian, *Talanta*, 2015, **141**, 47–52.
149 W. Chen, L. Hong, A.-L. Liu, J.-Q. Liu, X.-H. Lin and X.-H. Xia, *Talanta*, 2012, **99**, 643–648.
150 H. Jia, D. Yang, X. Han, J. Cai, H. Liu and W. He, *Nanoscale*, 2016, **8**, 5938–5945.
151 Q. Zhong, Y. Chen, X. Qin, Y. Wang, C. Yuan and Y. Xu, *Microchim. Acta*, 2019, **186**, 161.
152 P. Zhang, D. Sun, A. Cho, S. Weon, S. Lee, J. Lee, J. W. Han, D.-P. Kim and W. Choi, *Nat. Commun.*, 2019, **10**, 940.
153 Y.-W. Bao, X.-W. Hua, H.-H. Ran, J. Zeng and F.-G. Wu, *J. Mater. Chem. B*, 2019, **7**, 296–304.
154 S. Zhu, X.-E. Zhao, J. You, G. Xu and H. Wang, *Analyst*, 2015, **140**, 6398–6403.
155 G.-L. Wang, X. Xu, X. Wu, G. Cao, Y. Dong and Z. Li, *J. Phys. Chem. C*, 2014, **118**, 28109–28117.
156 T. Zhan, J. Kang, X. Li, L. Pan, G. Li and W. Hou, *Sens. Actuators, B*, 2018, **255**, 2635–2642.
157 J. Wang, F. Huang, X. Wang, Y. Wan, Y. Xue, N. Cai, W. Chen and F. Yu, *Process Biochem.*, 2019, **83**, 35–43.

158 H. J. Cheon, M. D. Adhikari, M. Chung, T. D. Tran, J. Kim and M. I. Kim, *Adv. Healthcare Mater.*, 2019, **8**, 1801507.
159 X. Cheng, L. Huang, X. Yang, A. A. Elzatahry, A. Alghamdi and Y. Deng, *J. Colloid Interface Sci.*, 2019, **535**, 425–435.
160 H. Zou, D. Tian, C. Lv, S. Wu, G. Lu, Y. Guo, Y. Liu, Y. Yu and K. Ding, *J. Mater. Chem. B*, 2020, **8**, 1008–1016.
161 I. Nath, J. Chakraborty and F. Verpoort, *Chem. Soc. Rev.*, 2016, **45**, 4127–4170.
162 X. Liu, Z. Yan, Y. Zhang, Z. Liu, Y. Sun, J. Ren and X. Qu, *ACS Nano*, 2019, **13**, 5222–5230.
163 M. Aghayan, A. Mahmoudi, S. Sohrabi, S. Dehghanpour, K. Nazari and N. Mohammadian-Tabrizi, *Anal. Methods*, 2019, **11**, 3175–3187.
164 Y. Pan, Y. Pang, Y. Shi, W. Zheng, Y. Long, Y. Huang and H. Zheng, *Microchim. Acta*, 2019, **186**, 213.
165 G. C. Ilacas, A. Basa, K. J. Nelms, J. D. Sosa, Y. Liu and F. A. Gomez, *Anal. Chim. Acta*, 2019, **1055**, 74–80.
166 Y.-L. T. Ngo, P. L. Nguyen, W. M. Choi, J. S. Chung and S. H. Hur, *Mater. Res. Bull.*, 2020, 110910.
167 Z. Taleat, A. Khoshroo and M. Mazloum-Ardakani, *Microchim. Acta*, 2014, **181**, 865–891.
168 F. Arduini, L. Micheli, D. Moscone, G. Palleschi, S. Piermarini, F. Ricci and G. Volpe, *TrAC, Trends Anal. Chem.*, 2016, **79**, 114–126.
169 T. R. de Oliveira, W. T. Fonseca, G. de Oliveira Setti and R. C. Faria, *Talanta*, 2019, **195**, 480–489.
170 M. U. Ahmed, M. M. Hossain, M. Safavieh, Y. L. Wong, I. A. Rahman, M. Zourob and E. Tamiya, *Crit. Rev. Biotechnol.*, 2016, **36**, 495–505.
171 J. Pla-Tolós, Y. Moliner-Martinez, C. Molins-Legua and P. Campins-Falcó, *Sens. Actuators, B*, 2016, **231**, 837–846.
172 J. Lai, Y. Yi, P. Zhu, J. Shen, K. Wu, L. Zhang and J. Liu, *J. Electroanal. Chem.*, 2016, **782**, 138–153.